NAVAL POSTGRADUATE SCHOOL

MONTEREY, CALIFORNIA

THESIS

EXAMINATION OF FLOW AROUND SECOND-GENERATION CONTROLLED-DIFFUSION COMPRESSOR BLADES IN CASCADE AT STALL

by

Kevin D. Fitzgerald

June 2004

Thesis Advisor:	Garth V. Hobson
Second Reader:	Raymond P. Shreeve

Approved for public release; distribution is unlimited

THIS PAGE INTENTIONALLY LEFT BLANK

REPORT DOCUMENTATION PAGE | *Form Approved OMB No. 0704-0188*

1. AGENCY USE ONLY *(Leave blank)*	**2. REPORT DATE** June 2004	**3. REPORT TYPE AND DATES COVERED** Master's Thesis

4. TITLE AND SUBTITLE: Examination of Flow Around Second-Generation Controlled Diffusion Compressor Blades in Cascade at Stall

5. FUNDING NUMBERS

6. AUTHOR(S) Fitzgerald, Kevin D

7. PERFORMING ORGANIZATION NAME(S) AND ADDRESS(ES)
Naval Postgraduate School
Monterey, CA 93943-5000

8. PERFORMING ORGANIZATION REPORT NUMBER

9. SPONSORING /MONITORING AGENCY NAME(S) AND ADDRESS(ES)
N/A

10. SPONSORING/MONITORING AGENCY REPORT NUMBER

11. SUPPLEMENTARY NOTES The views expressed in this thesis are those of the author and do not reflect the official policy or position of the Department of Defense or the U.S. Government.

12a. DISTRIBUTION / AVAILABILITY STATEMENT
Approved for Public Release; Distribution is Unlimited

12b. DISTRIBUTION CODE

13. ABSTRACT (maximum 200 words)

The flow around second-generation controlled-diffusion blades in cascade at stall was examined experimentally through the use of a two-component laser-Doppler velocimeter. Blade surface pressure measurements were also preformed at mid span on the blades at various Reynolds numbers. Flow visualization techniques were used to observe and record the flow on the surface of the blade. A correlation between the experimental results and computational fluid dynamic predictions was attempted in order to determine the exact nature of the flow as the blades approached stall, to further assist in the development of advanced blade design. The blade surface pressure measurements showed that the mid-span section of the blade was at a lower loading than previously measured at a smaller inlet flow angle. This indicated that the blade section was at stall. The flow visualization highlighted the extent of the three-dimensional flow over the blades. The LDV measurements documented the mid-span boundary layer and wake profiles.

14. SUBJECT TERMS
Controlled-Diffusion, Compressor, Stator, Cascade, Turbomachinery, Laser Doppler Velocimetry

15. NUMBER OF PAGES 77

16. PRICE CODE

17. SECURITY CLASSIFICATION OF REPORT	**18. SECURITY CLASSIFICATION OF THIS PAGE**	**19. SECURITY CLASSIFICATION OF ABSTRACT**	**20. LIMITATION OF ABSTRACT**
Unclassified	Unclassified	Unclassified	UL

NSN 7540-01-280-5500

Standard Form 298 (Rev. 2-89)
Prescribed by ANSI Std. 239-18

THIS PAGE INTENTIONALLY LEFT BLANK

Approved for public release; distribution is unlimited

EXAMINATION OF FLOW AROUND SECOND-GENERATION CONTROLLED DIFFUSION COMPRESSOR BLADES IN CASCADE AT STALL

Kevin D. Fitzgerald
Ensign, United States Navy
B.S.M.E., Georgia Institute of Technology, 2002

Submitted in partial fulfillment of the
requirements for the degree of

MASTER OF SCIENCE IN MECHANICAL ENGINEERING

from the

NAVAL POSTGRADUATE SCHOOL
June 2004

Author: Kevin D. Fitzgerald

Approved by: Garth V. Hobson
Thesis Advisor

Raymond P. Shreeve
Second Reader

Anthony J. Healey
Chairman, Department of
Mechanical and Astronautical Engineering

THIS PAGE INTENTIONALLY LEFT BLANK

ABSTRACT

The flow around second-generation controlled-diffusion blades in cascade at stall was examined experimentally through the use of a two-component laser-Doppler velocimeter. Blade surface pressure measurements were also preformed at mid span on the blades at various Reynolds numbers. Flow visualization techniques were used to observe and record the flow on the surface of the blade. A correlation between the experimental results and computational fluid dynamic predictions was attempted in order to determine the exact nature of the flow as the blades approached stall, to further assist in the development of advanced blade design. The blade surface pressure measurements showed that the mid-span section of the blade was at a lower loading than previously measured at a smaller inlet flow angle. This indicated that the blade section was at stall. The flow visualization highlighted the extent of the three-dimensional flow over the blades. The LDV measurements documented the mid-span boundary layer and wake profiles.

THIS PAGE INTENTIONALLY LEFT BLANK

TABLE OF CONTENTS

LIST OF FIGURES

THIS PAGE INTENTIONALLY LEFT BLANK

I. INTRODUCTION

A. BACKGROUND

As aircraft technology continues to advance so does the requirement for lighter, smaller and more efficient engines. These engines require increased blade loading, enhanced performance, and a wider range of usable conditions.

Compressor stall can lead to decreased engine performance if not complete loss of power from the engine. Ongoing research in the area of airfoil design has resulted in the ability to apply higher loads to the blades with increased efficiency; however this usually results in lower stall margins. Hence the ability of computer code to predict stall is imperative. These codes need to be calibrated against experimental data around the blades at stall. This requirement is the motivation for the present study.

The design of controlled diffusion blades is centered around the ability of the adverse pressure gradients to prevent boundary layer separation from occurring on the suction side of the blade. This allows for increased flow turning and high levels of blade loading or stage pressure rise. Alternatively the same pressure rise can be achieved with fewer blades, in turn reducing engine weight. Controlled-diffusion blade types were made possible through the development of Computational Fluid Dynamics (CFD), which allows the flow through various blade shapes to be modeled through the use of computers.

The controlled-diffusion blades examined were designed by Thomas F. Gelder of the NASA Glenn Research Center, formally NASA Lewis [Ref 1]. The current blades, Stator 67B, are a second-generation improvement of the Stator 67A blades designed by Nelson Sanger [Ref 2]. The stator 67B blades in conjunction with Rotor 67 form compressor stage 67B. Ten mid-span Stator 67B blades were examined in the Low-Speed Cascade Wind Tunnel at the Turbopropulsion Laboratory at the Naval Postgraduate School, located in Monterey, California.

B. PURPOSE

The objective of the current investigation was to further characterize the flow around these blades at a high angle of incidence, to both understand the flow and provide validation data for CFD modeling. In a previous study Hansen [Ref 3] examined mid-span conditions at a near design inlet flow angle of 36.3 degrees, this was done through the use of Laser-Doppler Velocimetry (LDV) and pressure probe measurements. Schnorenberg [Ref 4] examined the effect of Reynolds number on the separation region at an off-design, inlet flow angle of 38 degrees through the use of LDV measurements, flow visualizations and surface pressure measurements. Nicholls [Ref 7] preformed tunnel calibration following a motor replacement with five-hole probe, surface pressure and LDV measurements. Carlson [Ref 5] examined end-wall flow through the blades with five-hole probe measurements, LDV, and CFD. Caruso [Ref 6] examined the three-dimensional effects of corner vortices in the wake region at an off design inlet flow angle of 40.0 degrees with a three-component LDV system. The purpose of the present study was to examine the flow at the increased inlet flow angle of 40.5 degrees, which would likely result in a more complete stall.

II. APPARATUS AND INSTRUMENTATION

A. LOW-SPEED CASCADE WIND TUNNEL

This study was conducted in the Low-Speed Cascade Wind Tunnel (LSCWT) and Figure 1 depicts a schematic of the cascade in the Low Speed Turbomachinery Building. The specific aspects of the tunnel remain as previous documented by Nicholls [Ref 7]

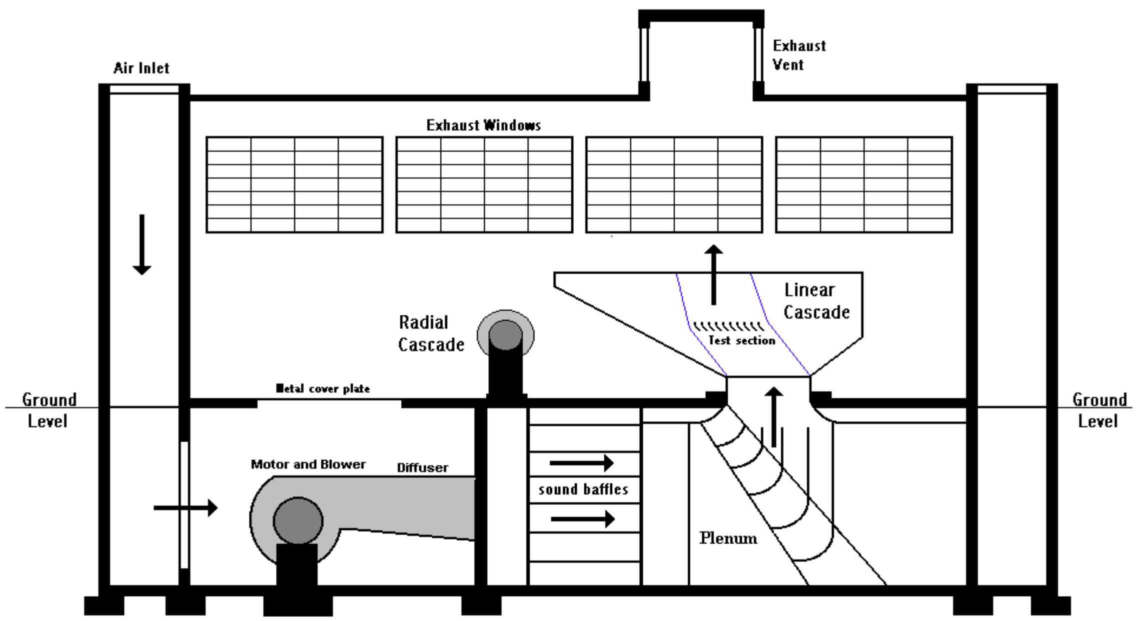

Figure 1. NPS Cascade Wind Tunnel Facility [From Ref. 6]

B. TEST SECTION

The test section of the LSCWT contained 10 Stator 67B controlled diffusion blades. The installation of the blades was documented by Hansen [Ref 3]. In Figure 2 it is possible to see a detailed layout of the cascade and the test section. Blade 1 in the test section was a “tufted” blade, blades 3, 4, and 5 were anodized black to aid in the LDV data collection. Blade 6 was the fully instrumented blade with 42 pressure taps used for the blade surface pressure measurements.

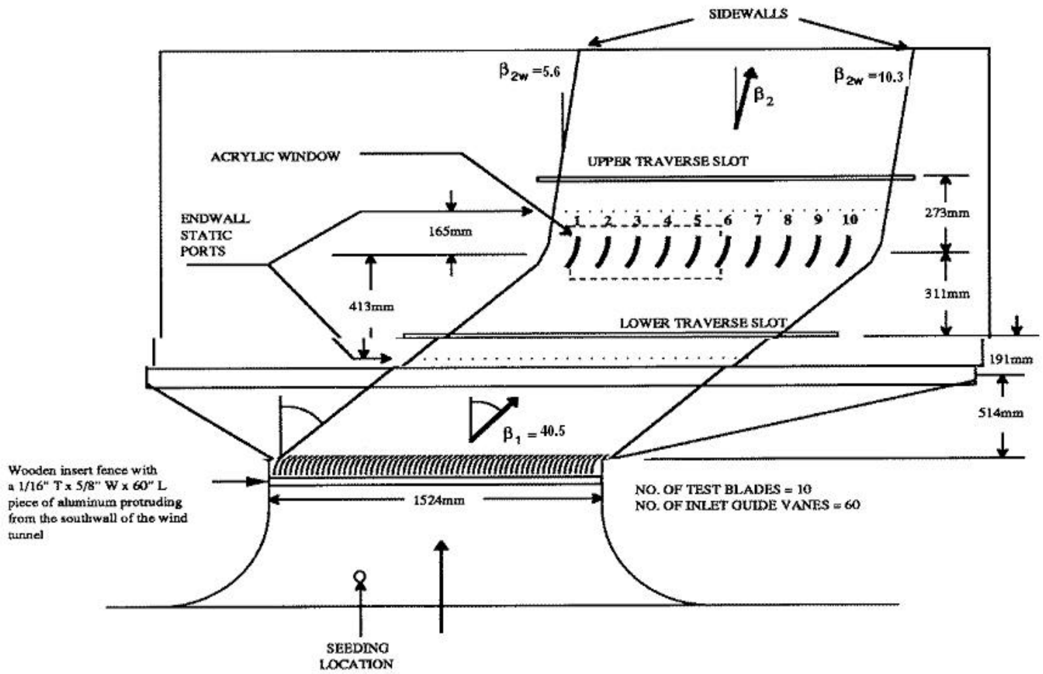

Figure 2. Test Section Schematic

The specific passage for the LDV measurements was between blades 3 and 4. The blade profile of a Stator 67B can be seen in Figure 3. Each blade had a span of 254 mm, was 127.25 mm in chord and the blade spacing was set to 152.4mm. Table 1 displays the specifics of the Stator 67B airfoil.

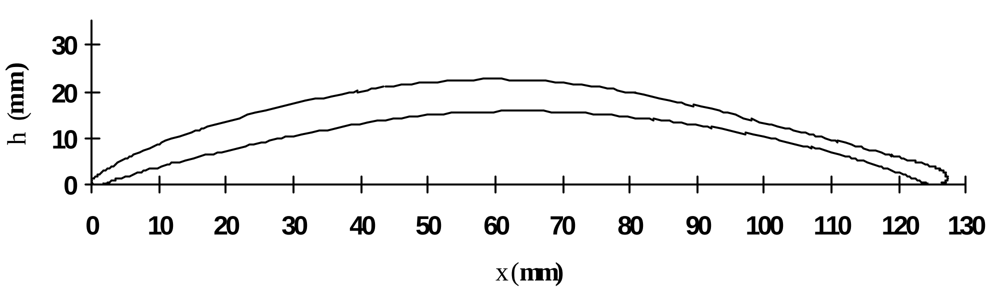

Figure 3. Stator 67B Blade Profile [From Ref. 6]

Table 1. Stator 67B Blade Characteristics

Type	Stator 67B Conrolled-Diffusion
Number of Blades	10
Spacing	152.4 mm
Chord	127.14 mm
Solidity	0.834
Thickness/Chord	0.05
Setting Angle	16.3 deg
Span	254.0 mm

A photograph of the 10 CD blades mounted in the test section of the LSCWT with the north wall of the tunnel removed is shown below in Figure 4.

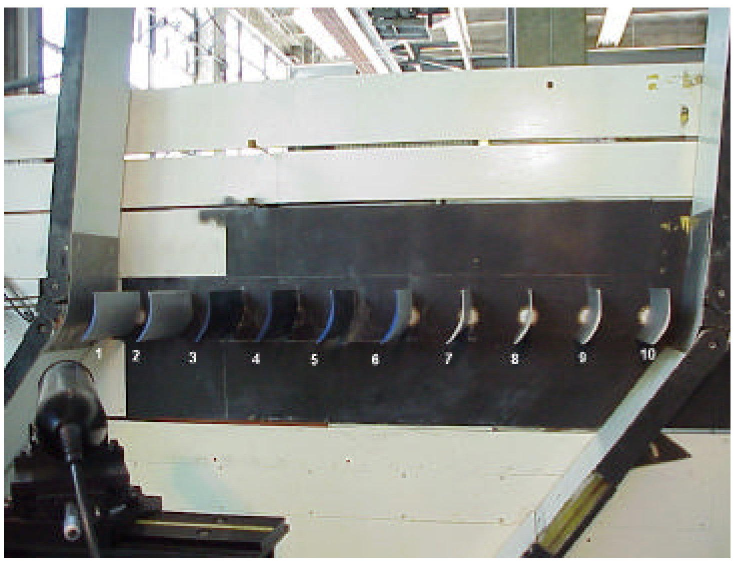

Figure 4. CD Blades Mounted in LSCWT

C. INSTRUMENTATION

1. Pressure Surveys

The surface pressure measurements were taken from the instrumented blade located at position 6. The pressure values were recorded using a 48 channel Scanivalve System that was controlled by a HP-VXI data acquisition system and a personal computer running HP-VEE software. A complete description of the data acquisition system can be found in Nichols [Ref 7]. Figure 6 is a picture of the fully instrumented blade prior to installation.

Figure 5. Instrumented Blade

2. Flow Visualization

Surface flow visualization was completed by mixing titanium dioxide (TiO_2) with kerosene which was in turn used to observe blade surface flow effects. The observations were documented with a digital video camera, capable of both video and still capture.

3. Laser-Doppler Velocimeter

The LDV system that was used in this experiment was a three-component fiber-optic system manufactured by TSI. The system can be broken down into four major sub-systems; the laser and optics, the data acquisition system, the traverse table and the seeding device.

a. Laser and Optics

The laser was a 4-Watt Lexel Argon-Ion laser. It was operated in a multi-line mode and was aligned so that it was emitted into a multicolor beam separator, a TSI model 9201 Colorburst as can be seen in Figure 6. The main beam was split into two beams to allow frequency shifting that aided in the data collection; these beams were referred to as the shifted and un-shifted beams. Each of these beams was then passed

through a prism that separated the two beams into three colored beams, one green (514 nm wavelength), one blue (488.0 nm wavelength) and one violet (476.5 nm wavelength). These beams were then transmitted via fiber optic cables to two probes. One probe was a single component probe receiving the violet beams, and other probe was a two-component probe receiving the green and blue beams. Each of these probes focused the respective beams at a point 349.8mm from the lens of the probes.

Figure 6. Argon-Ion Laser and Color Separator

b. Data Acquisition

The same probes that were used to focus the beams were also able to receive the scattered light from the seeded particles in the flow. The received scattered light was sent to a TSI Model 9230 Colorlink via a return fiber optic cable. The Colorlink in turn sent an electrical signal to the IFA 750 signal processor, which converted the Doppler burst into a digital frequency. The digital frequencies were then acquired by a PC via a multi channel interface and the TSI's FIND software version 1.4 was used to process the Doppler Signals. Figure 7 displays the Optical Probes, Traverse Table and Data Acquisition System.

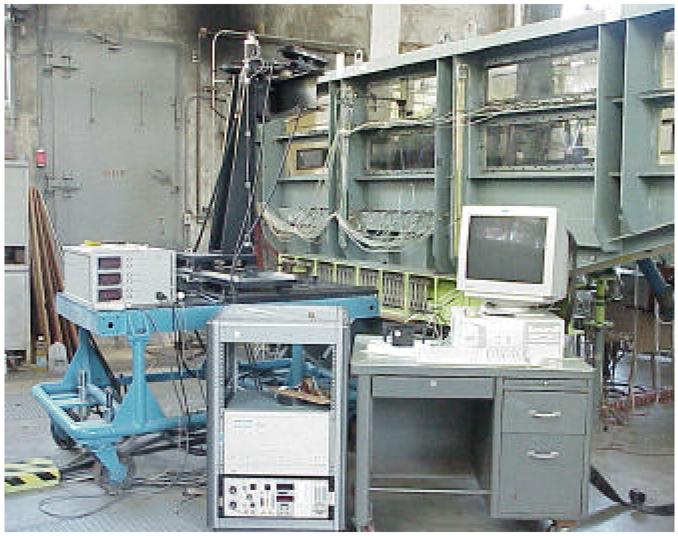

Figure 7. Optical Probes, Traverse Table and Data Acquisition System

c. Traverse Table

The two fiber optic probes were mounted on an “I” beam that was able to move independently in three directions; with a range of 600mm in all three. The table had the ability to be manually controlled but for a majority of the experiment the table was controlled via the FIND software.

d. Particle Seeding

An element vital to the success of the LDV system was the particle seeding. The seeding particles, approximately 1 micron in size, scattered the light from the laser beams, so that the Doppler effect could be measured. The size and location of the particles were important so that they properly followed the flow, and were focused where the beams were located. The particles were created by a TSI Model 9306 Six-Jet Atomizer using regular olive oil. The atomized particles were introduced upstream of the inlet guide vanes and the probe used to inject them could be rotated to effect the location of the particles in the flow. A picture of the atomizer and seeding probe can be seen in Figure 8.

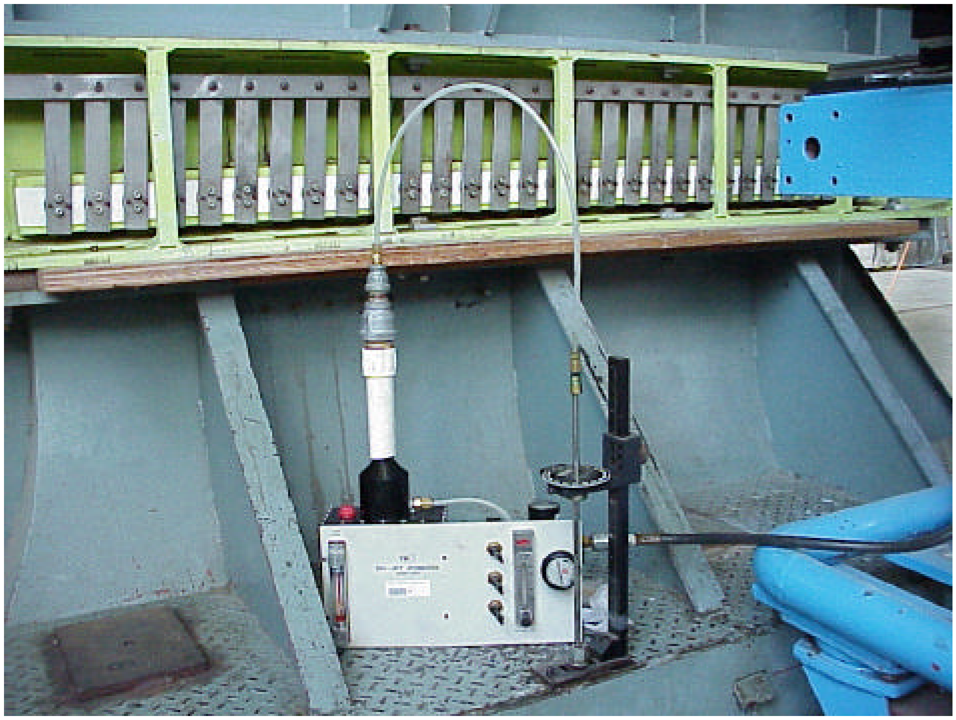

Figure 8. Six Jet Atomizer and Particle Seeding Probe

THIS PAGE INTENTIONALLY LEFT BLANK

III. EXPERIMENTAL PROCEDURES

A. PRESSURE MEASUREMENTS

The tunnel was allowed to stabilize at speed prior to data collection. Measurements were taken at blade 6 using a Scanivalve. Two complete runs were taken for data repeatability, measuring blade surface pressure on both the suction and pressure sides, in conjunction with plenum temperature and pressure. The data were collected done using the HP-VEE software called "Blade_Cp". The details of this program can be found in Reference 7.

B. FLOW VISUALIZATION

Surface flow visualization was preformed by removing the Plexiglas window on the tunnel and applying the TiO_2 Kerosene mixture to Blade 3. The tunnel was then run at the desired plenum pressure. Once the tunnel had stabilized the surface effects were recorded using a combination still and video digital camera.

C. LASER-DOPPLER VELOCIMETRY

Although the LDV system was a three-component system, only the two-component probe was used for these surveys. The blue and green pair of beams formed the probe volume used to measure the U and V components of the flow.

1. Laser Calibration and Probe Alignment

Initial alignment of the laser was required to ensure that the points used for the surveys were consistent, not only throughout the examination, but also so that the specific data could be directly compared to previous surveys. This was accomplished through the use of the alignment tool seen in Figure 9. The specifics of the alignment tool and the coordinate system can be found in Reference 3.

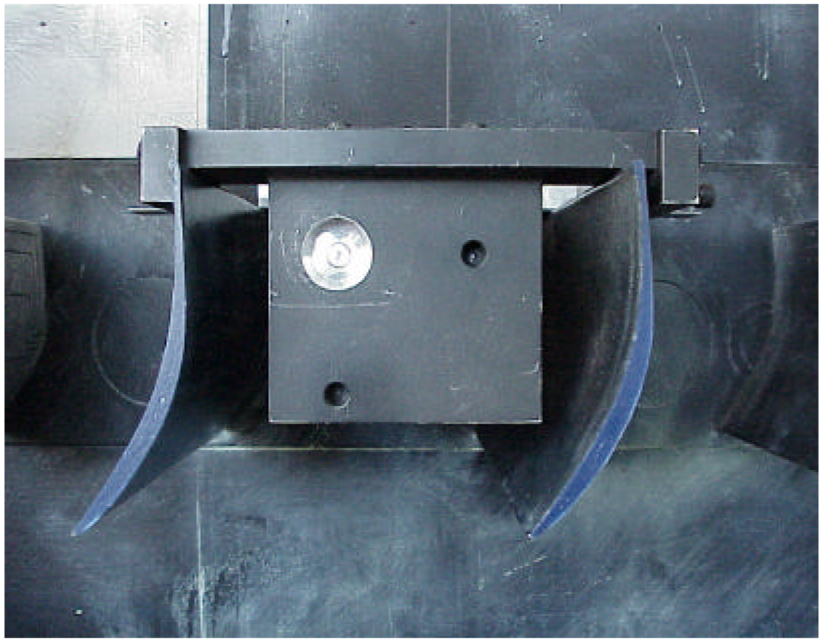

Figure 9. Alignment Tool Mounted in the Tunnel

Laser beam tuning was also performed whenever the laser was activated, to ensure that the relative power levels of the four beams were comparable. This was done to ensure that no one beam emitted a disproportional amount of light that would skew the ability of the probe to measure the scattered light from the other beams. This calibration was accomplished by adjusting the focusing lenses of the color separator for the specific beams.

2. Tunnel Calibration

The tunnel was calibrated by running the tunnel at five different levels. At each setting, plenum pressure, plenum temperature, and the atmospheric pressure were recorded for the tunnel, while the axial and tangential velocity components of the flow were measured at station 1. These data values were then entered into a FORTRAN program titled “CALIB1.FOR” to determine reference velocities which were used to non-dimensionalize the LDV data. The details of this program can be found in Reference 3.

3. Surveys

Three different types of surveys were performed; inlet surveys, wake surveys and boundary layer surveys. Inlet surveys were preformed at station 1, wake surveys were preformed at stations 11, 12, and 13. Boundary Layer surveys were preformed at stations 5bl-9bl. Figure 10 displays the locations of the boundary layer surveys and Figure 11 displays the station locations with respect to a blade mounted in the test section.

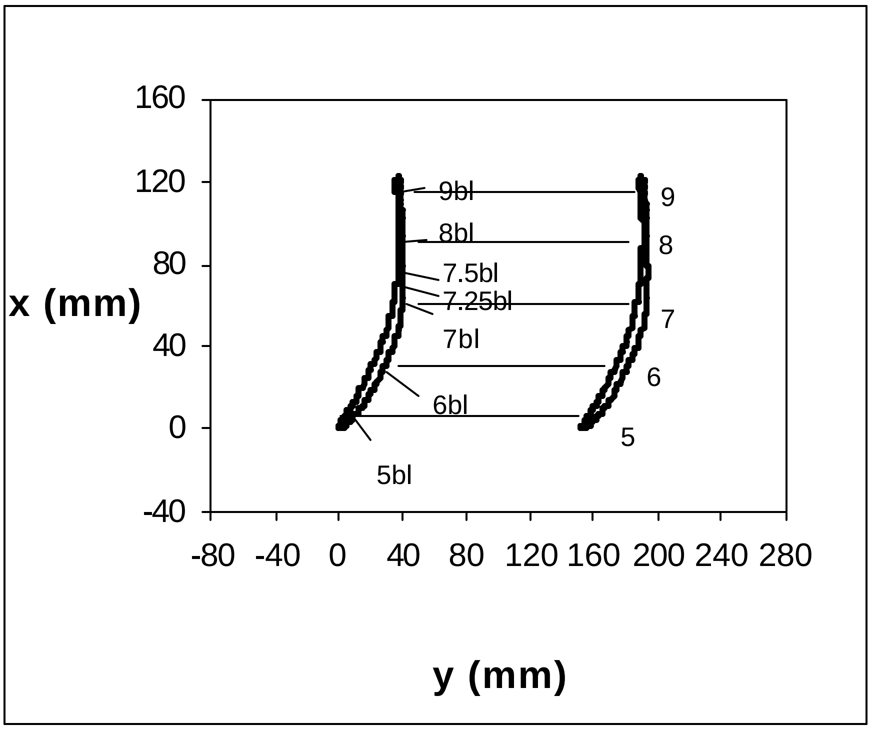

Figure 10. Boundary Layer Surveys

a. Inlet Surveys

The inlet surveys were preformed in order to determine the free-stream conditions upstream of the blades. Frequency shifting of 5 MHz was used for all inlet surveys, and the probe was positioned parallel to the tunnel window.

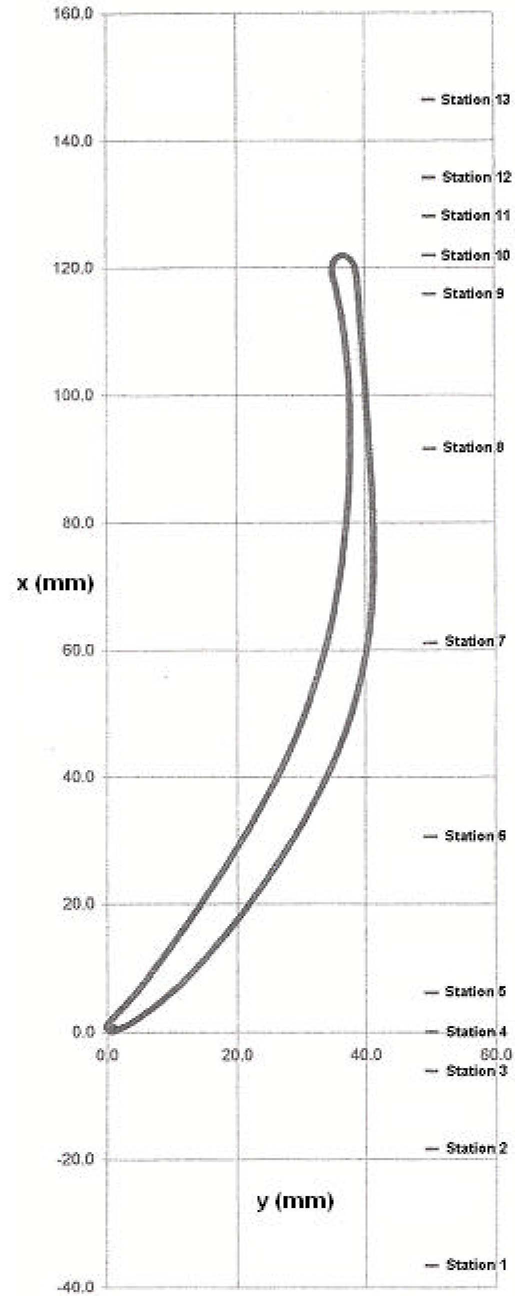

Figure 11. Laser-Doppler Survey Location

b. *Boundary Layer Surveys*

Boundary layer surveys were preformed at stations 5bl, 6bl, 7bl, 7.25bl, 7.5bl, 8bl, and 9bl. These surveys were preformed perpendicular to the suction side of the blade at the respective station points. Various levels of shifting were used throughout the surveys from 0 shifting to 10Mhz of shifting due to the backflow and shear layer

regions that existed in the boundary region. Only the axial component of the velocity was measured at stations 7bl-9bl. The tangential component could not be examined due to the reflection that occurred as the beams neared the blade and the blade itself reflected and scattered the light. At station 5bl and 6bl axial data were taken with the probe as described, and then the probe was rotated ninety degrees in order to facilitate the tangential data collection; then the probe was returned to its original location for further surveys. It was not possible to rotate the probe at station 7bl-9bl to record axial data, due to the camber of the blade at those stations. The probe was yawed 4 degrees from perpendicular to the window in order to allow the left-most beam to enter the tunnel parallel to the blade, and the intersection of the beams could occur right at the surface of the blade

c. Wake Surveys

Wake surveys were conducted to determine the nature of the flow downstream from the trailing edge. Combinations of shifting settings were used to complete the surveys. The shifting settings varied from 5Mhz for the free-stream areas to 2Mhz and 10Mhz in the wake from the tip of the blade. Again the probe was positioned perpendicular to the tunnel window.

THIS PAGE INTENTIONALLY LEFT BLANK

IV. RESULTS AND DISCUSSION

A. PRESSURE SURVEYS

Blade surface pressure measurements were taken on blade 6 for a Reynolds number of 640,000. The results of the measurements can be seen in Figure 12. This figure displays the results not only of the current measurements but also for the previous work performed by Nicholls [Ref 7], where the inlet-flow angle was set to be 40.0 degrees. The data in the figure are presented in terms of the coefficient of pressure, Cp, versus the fraction of blade chord, x/c.

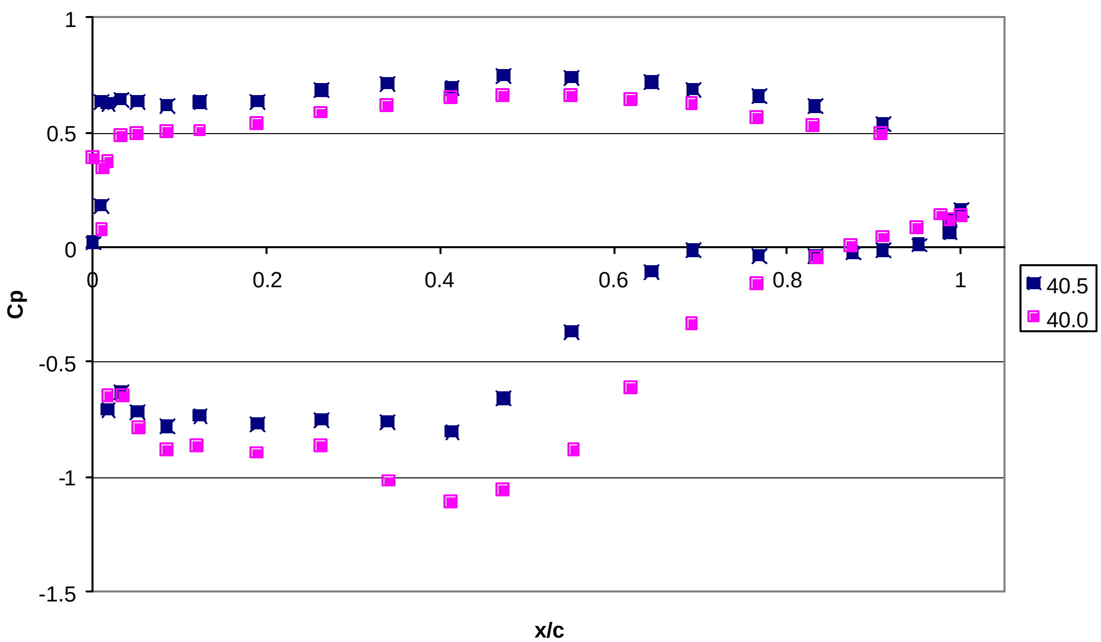

Figure 12. Pressure Distributions at Blade 6.

From the comparison of the current data with the data from the previous study it is possible to see the decrease in the area under the curve on the suction side of the blade. This results in a loss of lift with respect to the previous conditions that occurs along almost the entire suction side of the blade. It is also of interest to note that although the

pressure readings on the pressure side of the blade are similar, there is a significant difference on the suction side of the blade. The suction pressure peaks at 0.8 for the current study, but the previous study has a peak of 1.2 at x/c equal to 0.4. The suction pressure decreased to zero at x/c equal to 0.7, beyond which there was no pressure gradient which indicated the presence of separated flow or a region of reversed flow. Additional surface pressure measurements were taken at various Reynolds numbers. The plots of these data can be seen in Appendix A.

B. FLOW VISUALIZATION

Flow visualization was performed on blade 4, Figures 13 and 14 show the results of the visualization. Data were taken only after the effects were solely the results of the flow at speed, and not from the startup process. The vortices that formed on the corners of the blade were a result of the end-wall flow that occurred in the tunnel. In Figure 13 it is possible to observe the area of back flow that existed over most of the blade span from about x/c equal to 0.5 to the trailing edge. The reverse flow was due to the roll up of the two corner vortices that resulted in a region of flow separation between them. The non-symmetric nature of the flow was also evident from the flow visualization; a result of the differences of the end wall flow present in the tunnel. The separation line at mid span was at an approximate x/c of 0.6, which was slightly less than the separation indicated by the Cp data (Figure 12), which was at x/c of 0.7. The difference was attributed to the fact that there was a noticeable effect on the flow visualization due to gravity and therefore cannot be used as an absolute tool for the specific location of events occurring on the blade. Additional flow visualization for reference Reynolds numbers can be found in Appendix B.

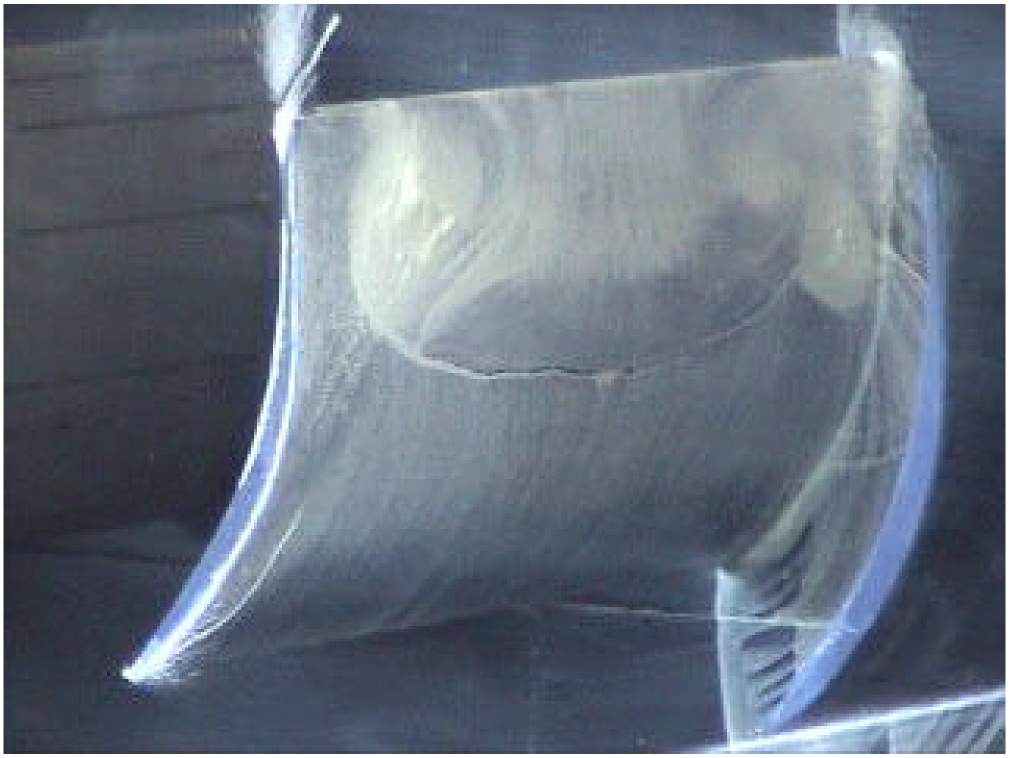

Figure 13. Blade Surface Flow Visualization

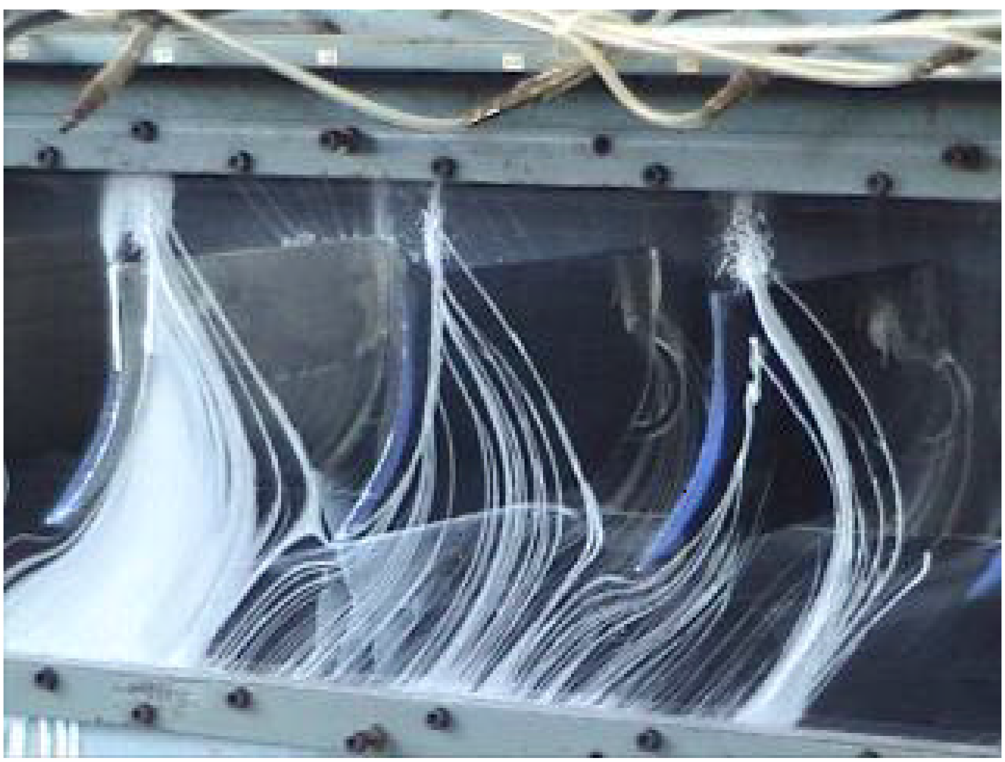

Figure 14. End-Wall Flow Visualization

C. LASER-DOPPLER VELOCIMETRY

1. Inlet Surveys

An inlet survey was preformed at station 1, the results of which can be seen in Figure 15. The velocity profile was fairly consistent throughout the survey, which was across one blade pitch or spacing. The slight sinusoidal nature of the velocity profile was attributed to the upstream potential effect of the blades on the flow, since the period of the variation was one blade pitch or spacing. Average axial turbulence was 1.5% and the average tangential turbulence was 1.7%. This data showed evidence of the unmixed inlet guide vanes wakes, which were more closely spaced (six per blade passage). The velocity data taken corresponded to a Reynolds number of 640,000 and a Mach number of 0.22. The recorded data for the survey can be found in Appendix C.

2. Boundary Layer Surveys

Boundary layer surveys were preformed at stations 5, 6, 7, 7.25, 7.5, 8, and 9. The results of the surveys can be seen in Figures 16-22, which present the non-dimensional velocity ratio (non-dimensionalized by V_{ref} which is defined in Appendix C), or turbulence intensity, versus d/c, where d is the distance from the blade surface and c is the blade chord. The yawing of the laser probe allowed data to be taken as close as possible to the blade; but it introduced a high level of reflected light as the beams approached the blade from the free stream during the survey. In some cases the combination of the camber of the blade and this yaw angle prevented two-component data being taken. The specific cases for each boundary layer survey follow. All the raw recorded data for these surveys can be found in Appendix C.

a. Station 5bl

The graphical results for the survey at station 5bl can be seen in Figure 16. At station 5bl is was possible to gather both U (tangential) and V (axial) component data. However, it had to be done in separate surveys due to the interference caused by reflected light from multiple beams. Figure 16 shows the normalized mean values of U, V, and W (combined), which were fairly constant in the free stream and only dropped off in

magnitude at d/c equal to 0.05, demonstrating that the boundary layer was attached at that station. The turbulence intensity peaked above 10% close to the blade surface and only leveled off at approximately a d/c equal to 0.06, which was an indication of the extent of the boundary layer.

b. Station 6bl

The graphical results for the survey at station 6bl can be seen in Figure 17. Station 6 was similar to that of station 5 in the sense that both tangential and axial components were recorded, but they had to be done separately. The velocity data again decreased close to the surface of the blade, however reflected and scattered light caused by a combination of the yaw of the laser and the camber of the blade prevented data from being taken closer then d/c equal to 0.16. Turbulence intensity profile peak occurred closest to the blade, and leveled off at approximately d/c equal to 0.04. These characteristics were of note due to the fact that the size of the boundary layer decreased.

c. Station 7bl

The graphical results for the survey at station 7bl can be seen in Figure 18. At station 7, and all of the following boundary layer stations, the camber of the blade prevented axial data from being recorded due to the reflection and back scattering that occurred. Here again the flow was attached, however the boundary layer profile showed signs of an inflection in slope close to the blade surface which was a precursor to flow separation. The turbulence intensity profile showed a peak of approximately 12% at a d/c equal to 0.015, which was off the blade surface, which also indicated the boundary layer was close to separation. The peak in turbulence intensity corresponded to the location of the maximum shear or velocity gradient in the mean velocity profile. A total of three surveys were required to complete an overall survey from the free stream to the surface of the blade. In Figure 18 the surveys labeled "U Mean 1" and "U mean 3" used frequency shifting of 2 MHZ and the survey labeled "U Mean 2" used frequency shifting of 5 MHz.

d. Station 7.25bl

The graphical results for the survey at station 7.25bl can be seen in Figure 19. Here again the flow was attached and demonstrated very similar characteristics to that of station 7bl, with respect to inflection in the velocity profile and peak turbulence

intensity occurring off the blade surface. The velocity profile shows that close to the blade surface negative values were recorded, consistent with the onset of separation prior to this station. Turbulence intensity values return to free-stream conditions at a d/c of approximately 0.05, which is higher then at station 7, further reinforcing the growth of the boundary layer and increased effect from the onset of separation. Multiple surveys were preformed because of problems with the FIND software; not simply for various levels of shifting.

e. Station 7.5bl

The graphical results for the survey at station 7.5bl can be seen in Figure 20. This survey demonstrated a classical reverse flow profile consistent with complete separation that occurred at or before station 7.25bl. There was an extensive region of back flow present from d/c of 0.1 to 0.25. The turbulence intensity profile had two peaks, both falling in the range of 16-18%. The first corresponded to the location of the transition from negative to positive flow, and the second corresponded to the location of the maximum shear, or velocity gradient, prior to returning to free-stream conditions. The double peaks are not consistent with two-dimensional separation; they may be a result of the complex three-dimensional separation that occurred over the blades. Again the use of multiple surveys was required due to software issues, and small inconsistencies between the surveys are present.

f. Station 8bl

The graphical results for the survey at station 8bl can be seen in Figure 21. Here the flow is clearly separated. The velocity profile exhibits portions of back flow close to the blade and then a transition to free-stream conditions. The turbulence graph has a similar double peak profile to that of station 7.5bl occurring at d/c values of 0.08 and 0.12 respectively and with values in the range of 16-18% and the second peak still corresponds to the location of maximum shear immediately prior to the return to free-stream conditions. Station 8 required the use of three separate surveys using frequency shifting values of 2 MHz for “U Mean 1” and “U Mean 3” and 5 MHz for “U Mean 2.”

g. Station 9bl

The graphical results for the survey at station 9bl can be seen in Figure 22. The velocity and turbulence intensity profiles are most clearly defined at station 9, due to

the distance from the point of separation. The velocity profile still is consistent with back flow, and is more exaggerated then it was at station 8bl. The turbulence intensity profile however no longer has a double peak, there is only one peak occurring at d/c of 0.15 and a magnitude of 22%. The location of this peak corresponds to the maximum shear location prior to the flow returning to free-stream conditions.

3. Wake Surveys

Wake surveys were preformed at stations 11, 12, and 13. For these surveys the probe was aligned perpendicular to the window. Due to the back flow regions that exist in the wake, various frequency shifting was used to gather the data. In the free-stream regions 5MHz frequency shifting was used; in the wake of the trailing edge on the suction side 10MHz frequency shifting was used; and in the wake of the trailing edge on the pressure side 2 MHz frequency shifting was used. The results of these surveys can be seen in Figures 23-25, which present the non-dimensional velocity ratio or turbulence intensity versus y/s, where y is the horizontal position and s is the blade span. In these surveys it was possible to measure tangential and axial components simultaneously in coincidence mode.

a. Station 11

The graphical results for the survey at station 11 can be seen in Figure 23. A fine resolution survey was preformed at station 11 in attempt to better measure the range in which back flow exists. From the velocity data it is possible to see the region of back flow that exists from approximately y/s of 0.25 to 0.38. The trailing edge of the blade was situated at approximately 0.25 y/s, demonstrating the region of back flow occurred primarily on the suction side. The turbulence intensity profile peaked in two areas at y/s of 0.23 and 0.39 with maximum magnitudes of approximately 16 and 20%, which corresponded to the maximum shear gradients on either side of the wake profile. The first major decrease in the flow that occurred near the trailing edge was expected but the abrupt shift in the V Mean velocity profile that occurred at y/s of 0.38 was unexpected.

b. Station 12

The graphical results for the survey at station 12 can be seen in Figure 24. The survey at station 12 was taken over multiple blade passages in order to show the periodicity of the recorded data, which was successful. Again the regions of back flow existed in and around the trailing edge of the blade as was observed at station 11. Here however, these regions are wider due to the additional distance from the trailing edge. The double peak profile was repeated over both passages, and occurred at the same values as at station 11, a y/s of 0.23 and 0.39 with maximum magnitudes of approximately 20%. The abrupt change in velocity values were no longer limited to the V Mean values but also were seen in the U Mean values at station 12.

c. Station 13

The graphical results for the survey at station 13 can be seen in Figure 25. Again the characteristics at station 13 are similar to those at the previous two stations, but the region of back flow did not exist at station 13. The peaks in the turbulence intensity occurred at the same points as they had at station 12, and 13, at y/s of 0.23 and 0.39, with maximum magnitudes of approximately 15 and 20%.

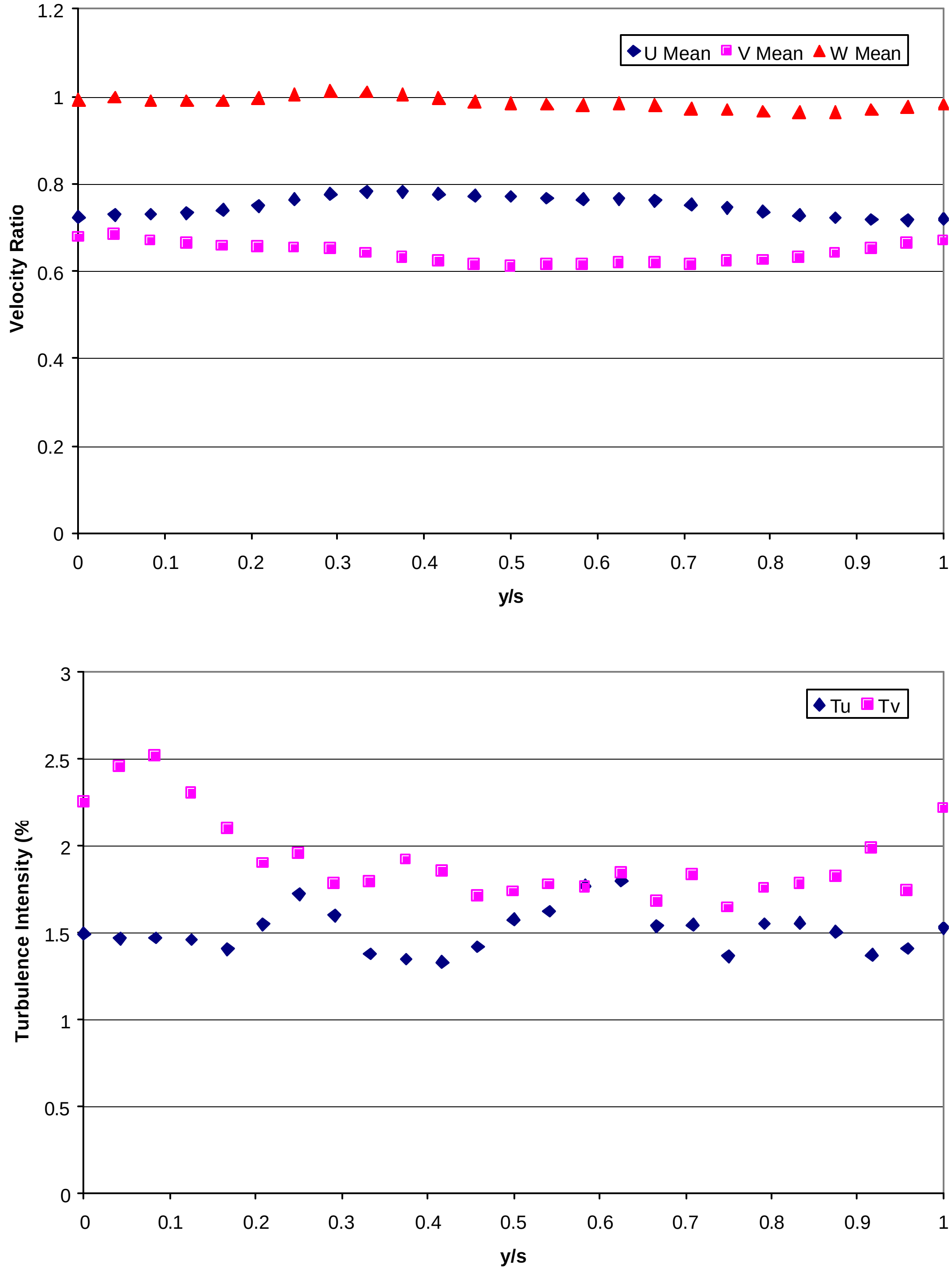

Figure 15. Station 1 Inlet Survey

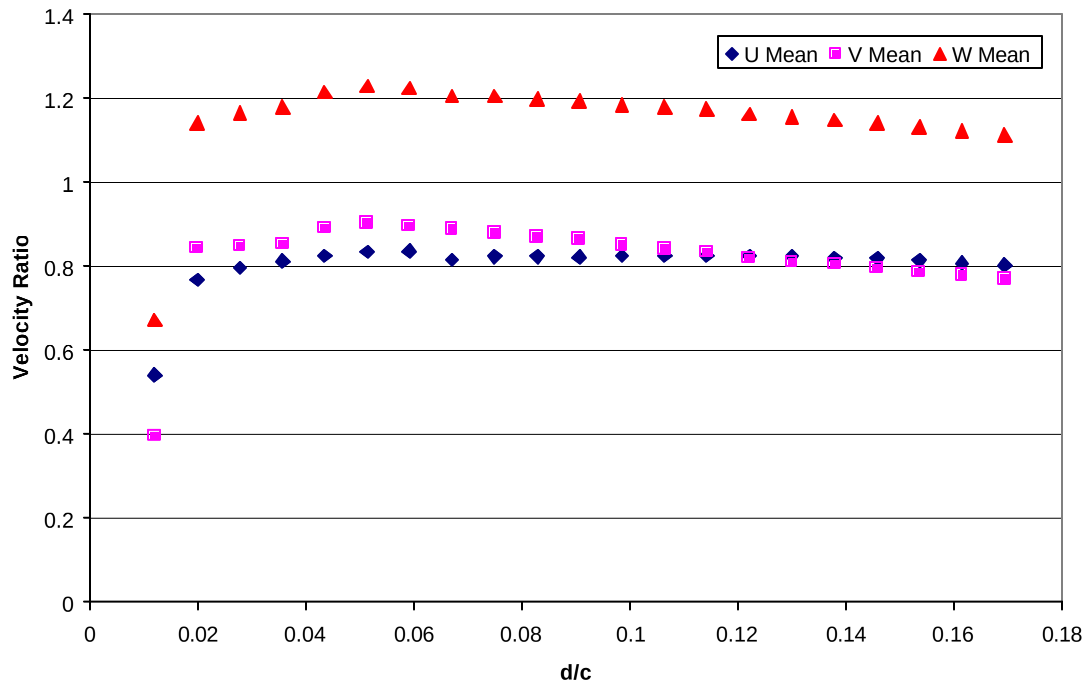

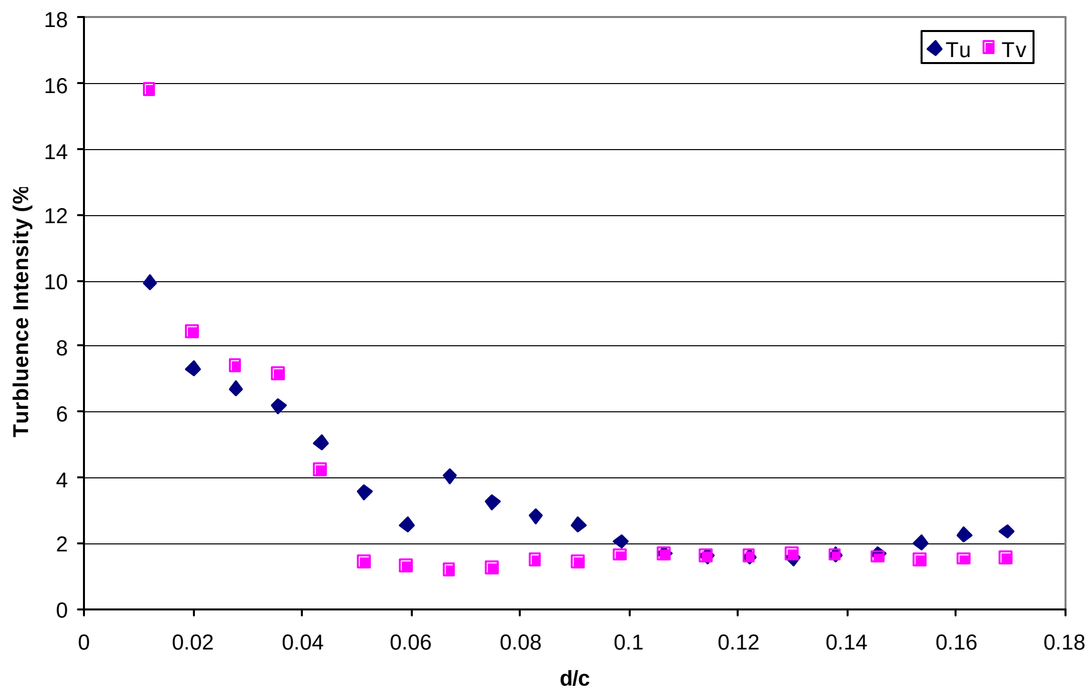

Figure 16. Station 5 Boundary Layer Survey

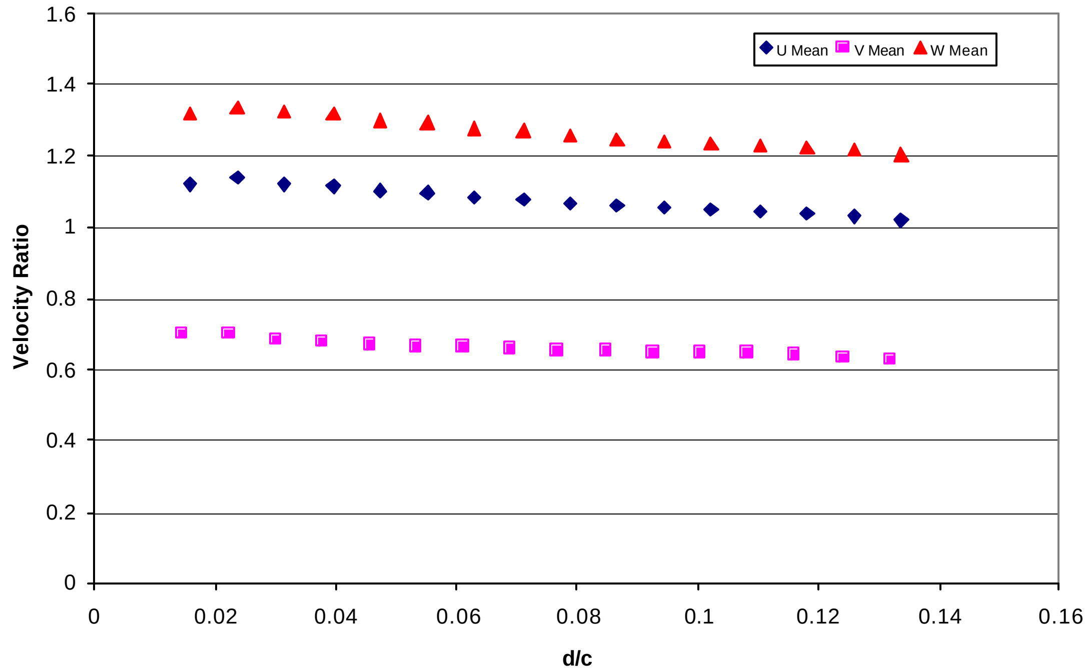

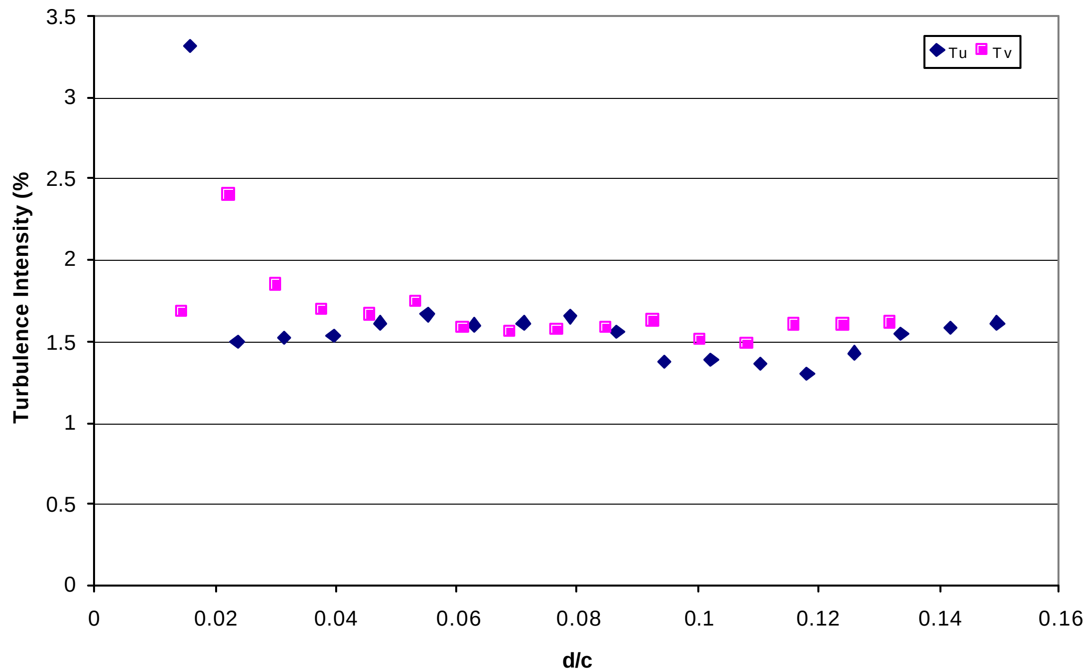

Figure 17. Station 6 Boundary Layer Survey

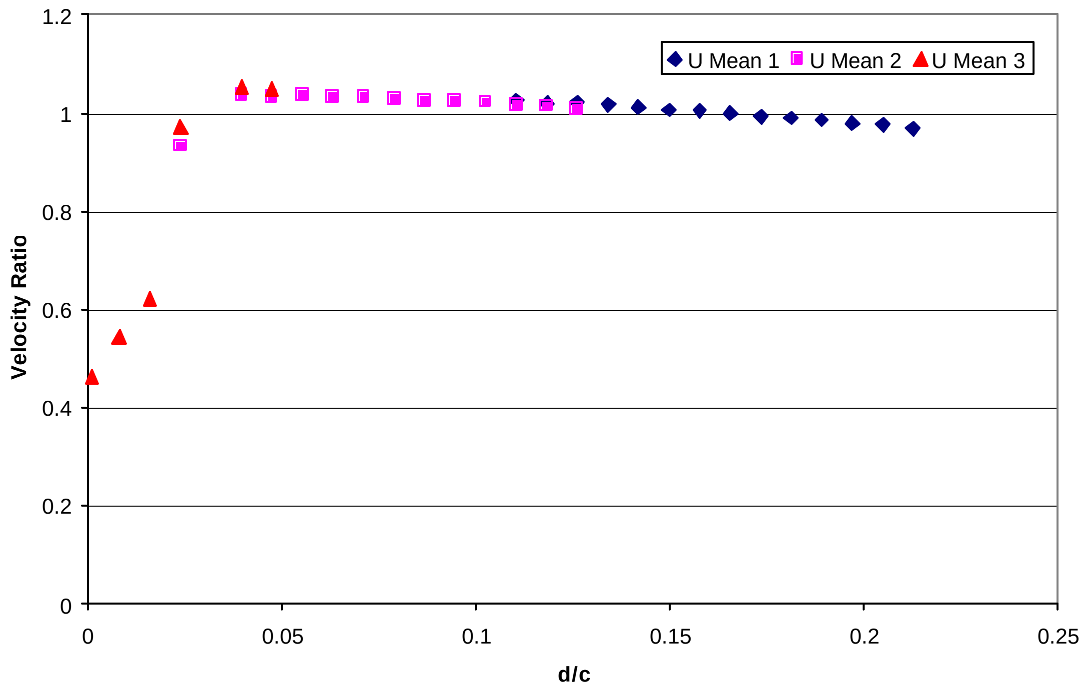

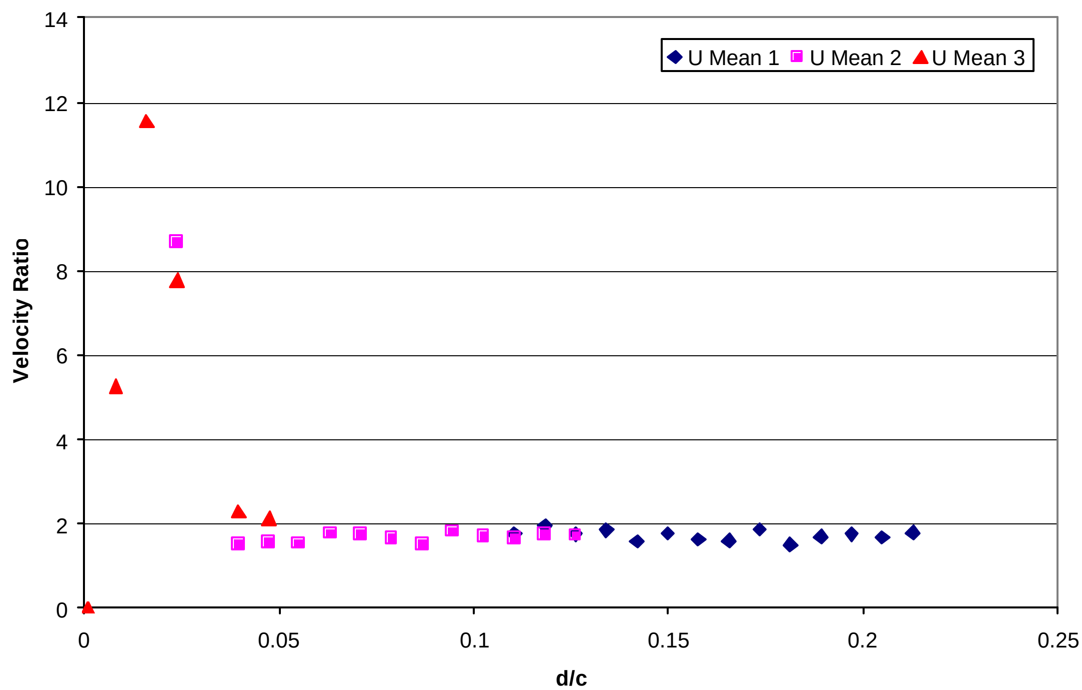

Figure 18. Station 7 Boundary Layer Survey

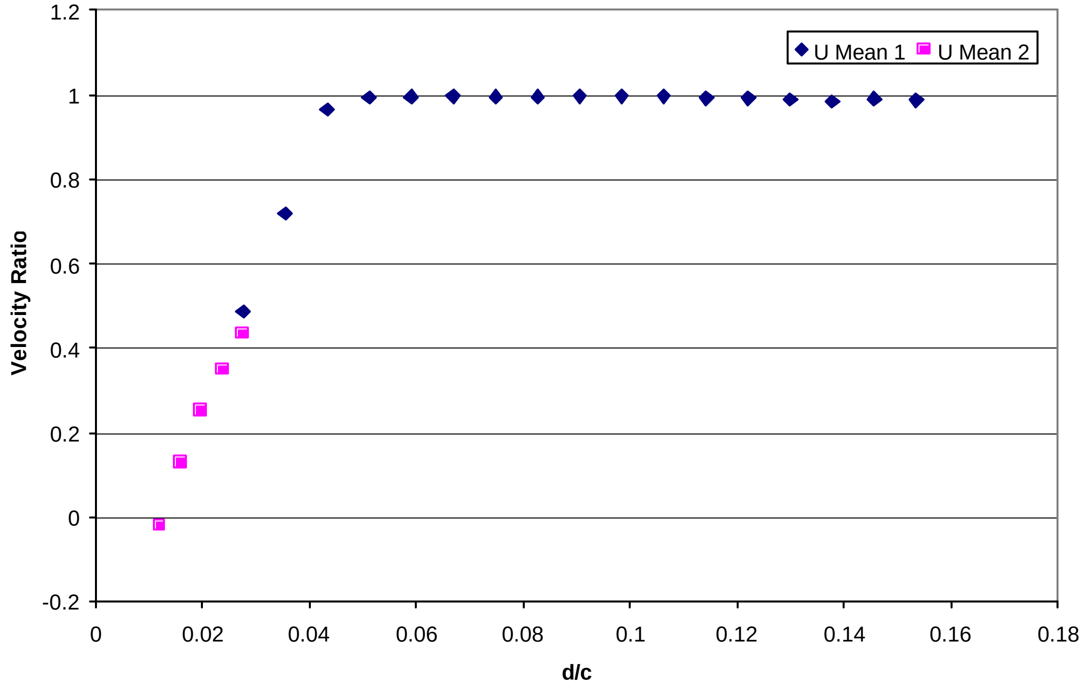

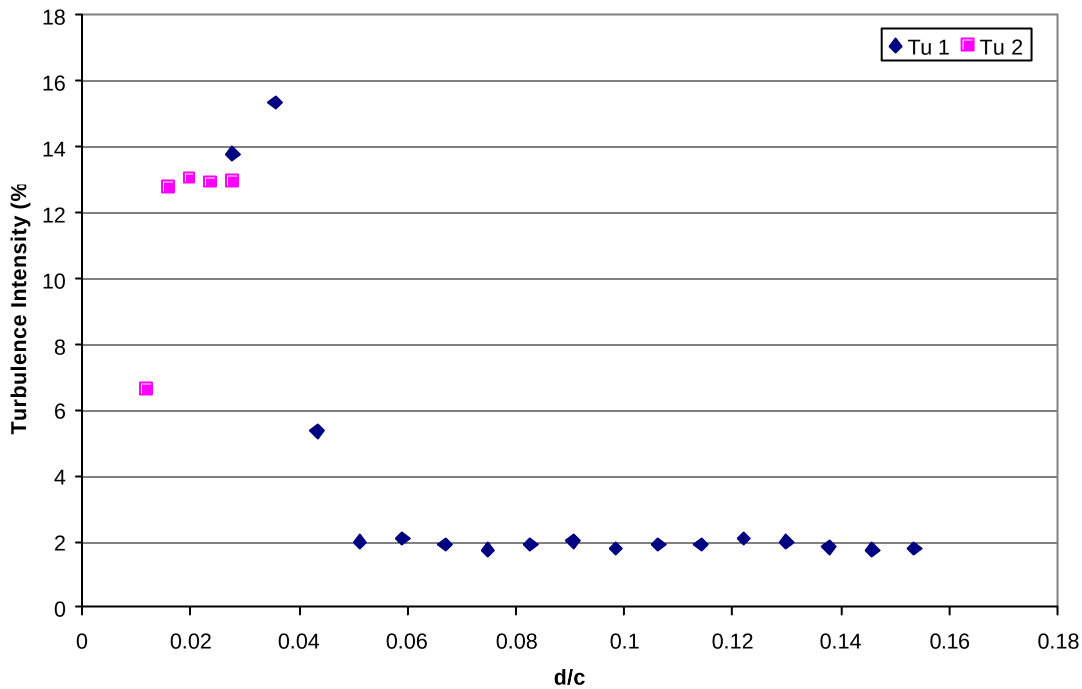

Figure 19. Station 7.25 Boundary Layer Survey

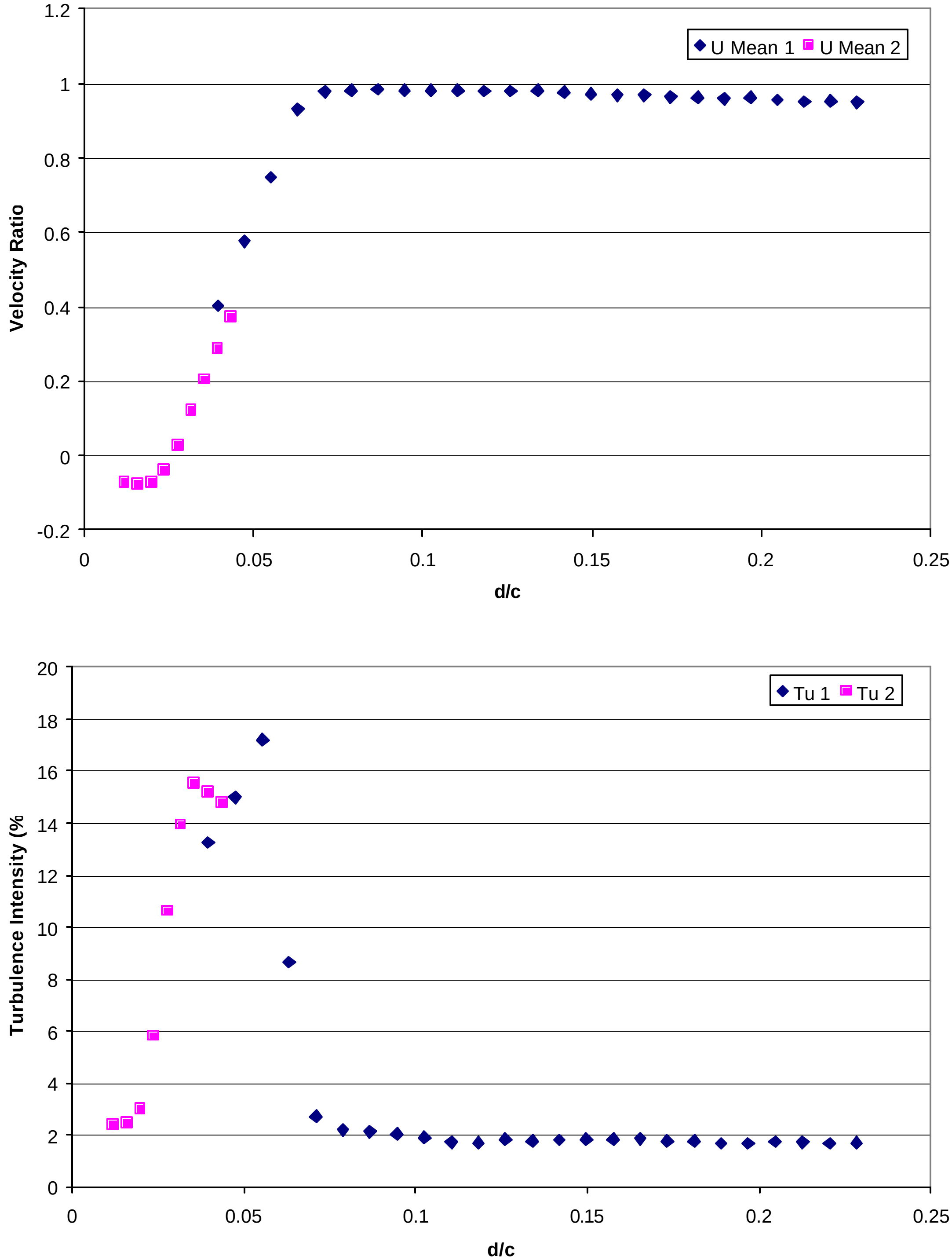

Figure 20. Station 7.5 Boundary Layer Survey

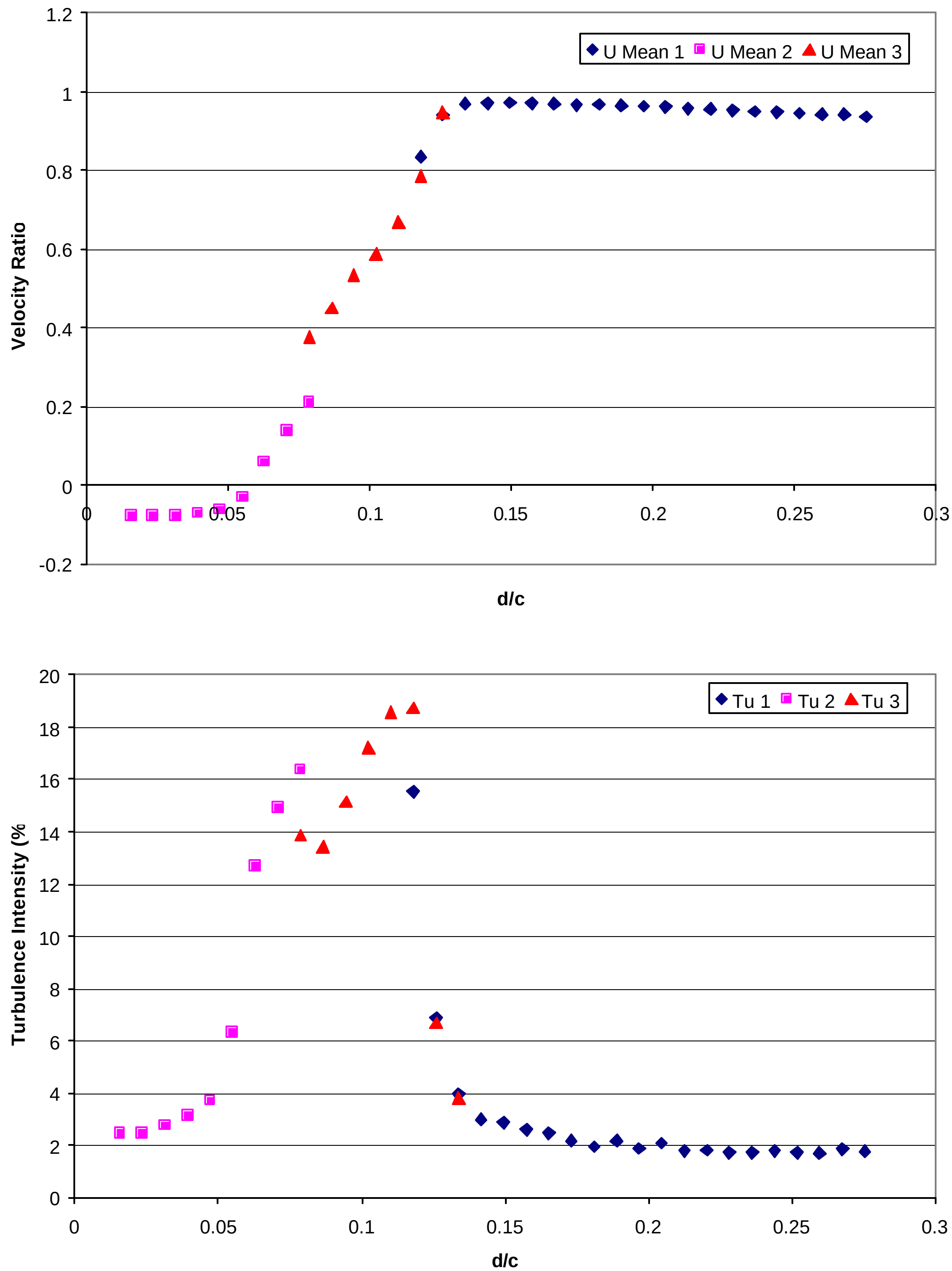

Figure 21. Station 8 Boundary Layer Survey

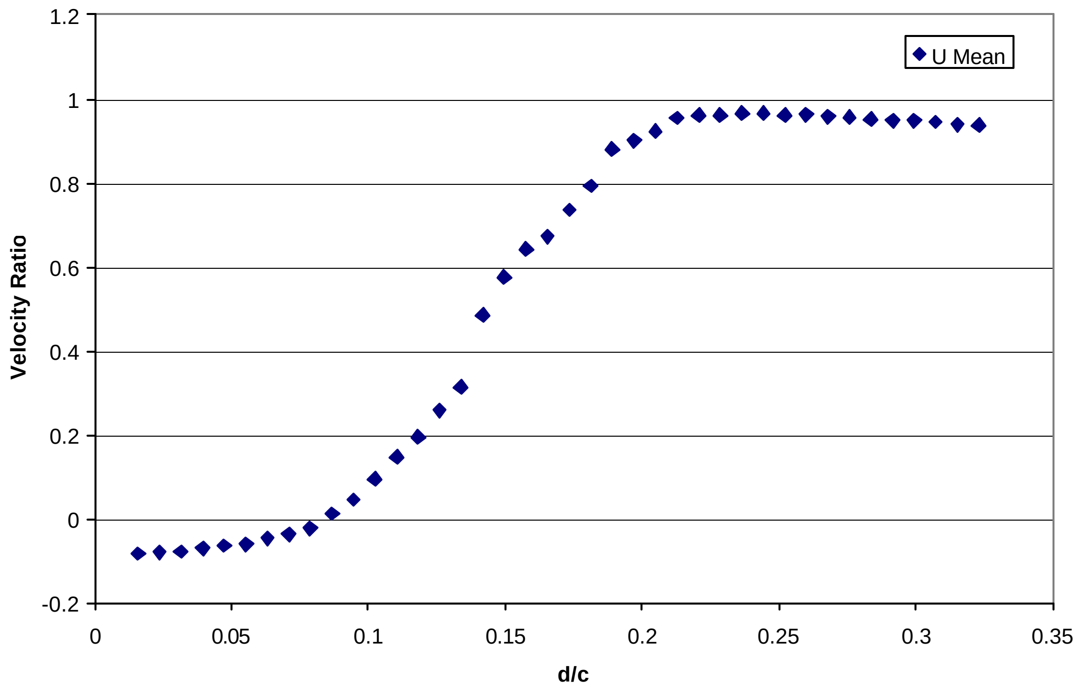

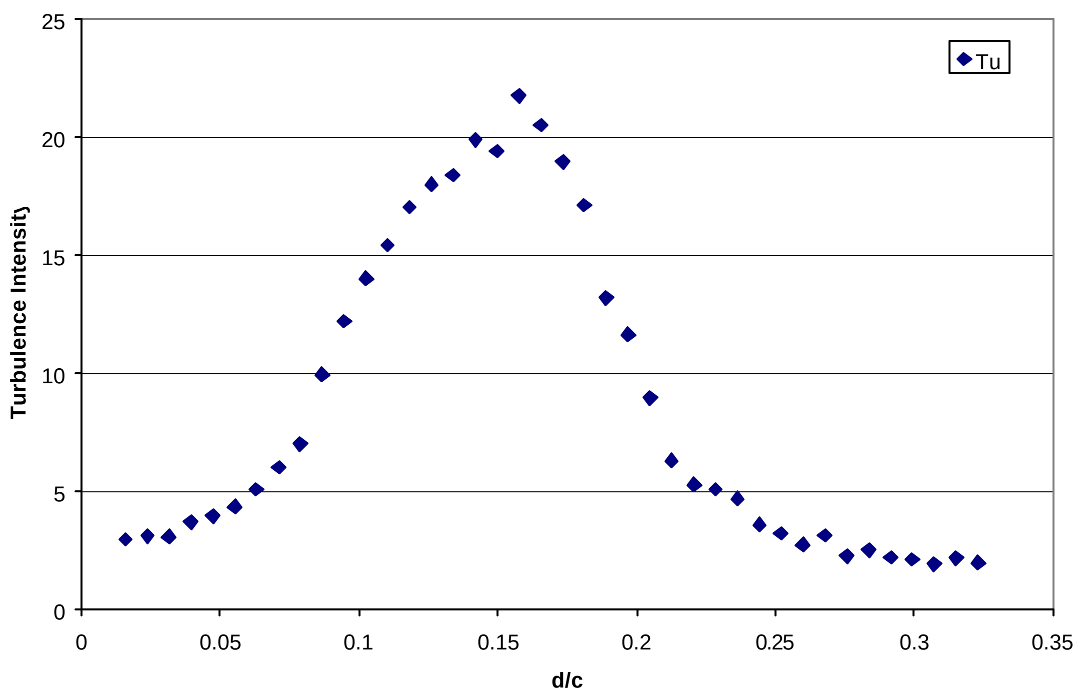

Figure 22. Station 9 Boundary Layer Survey

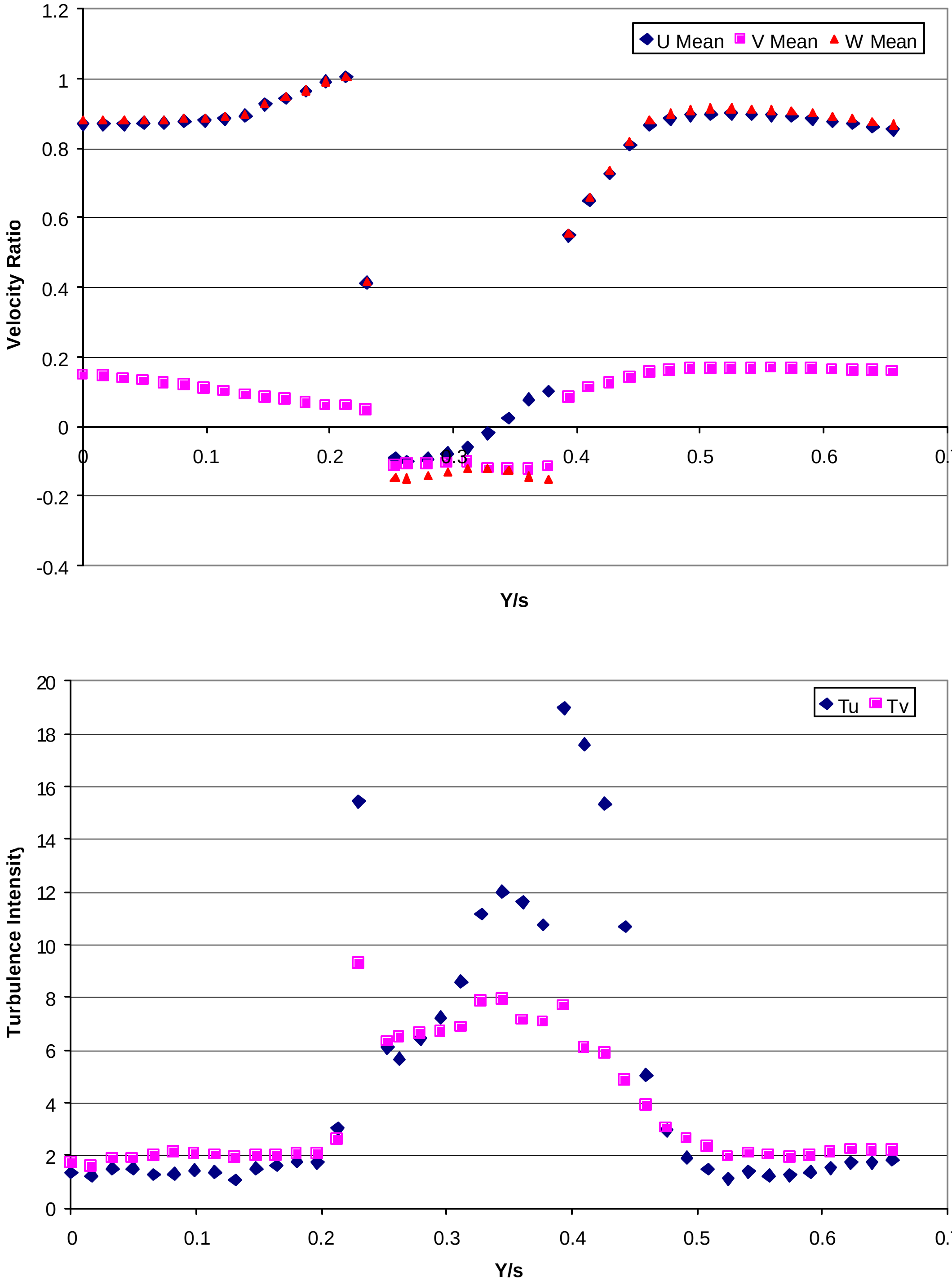

Figure 23. Station 11 Survey

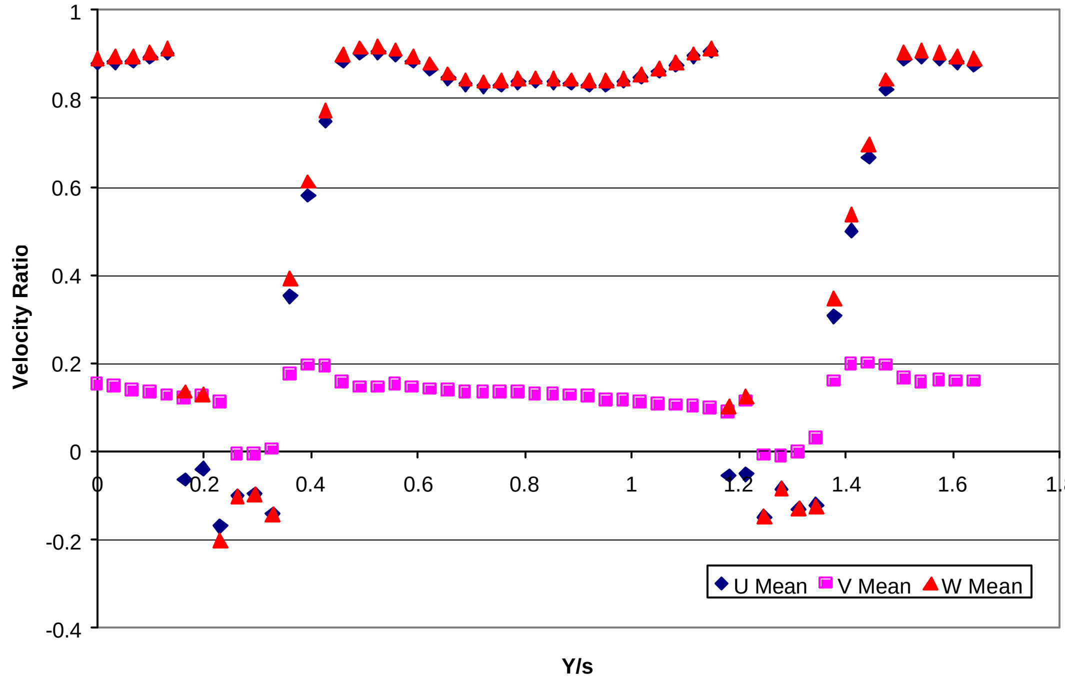

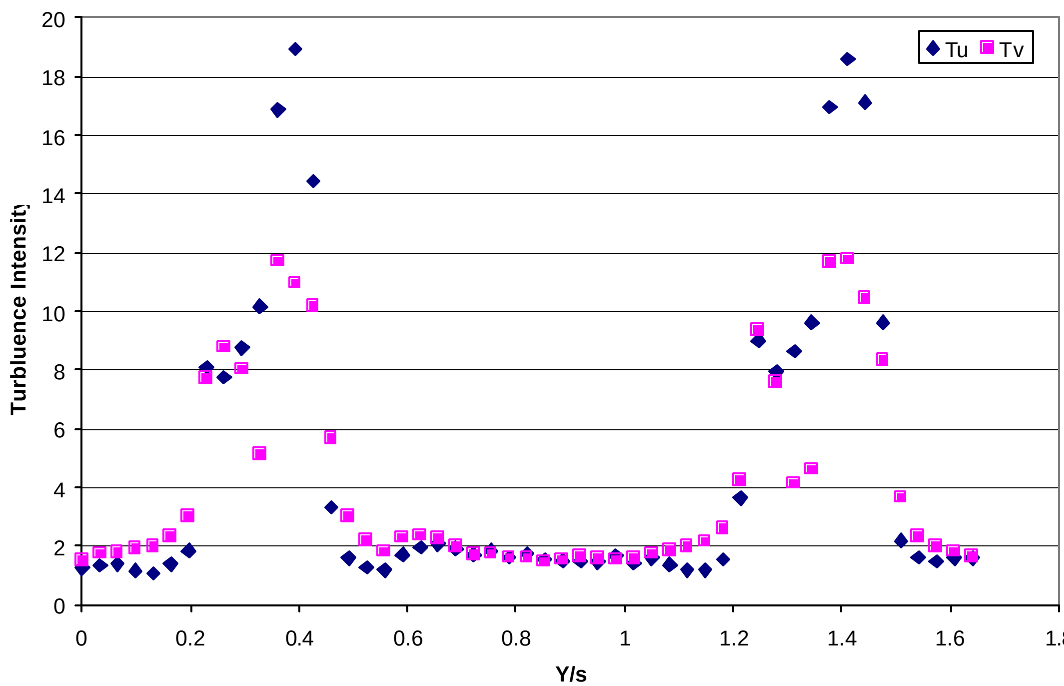

Figure 24. Station 12 Survey

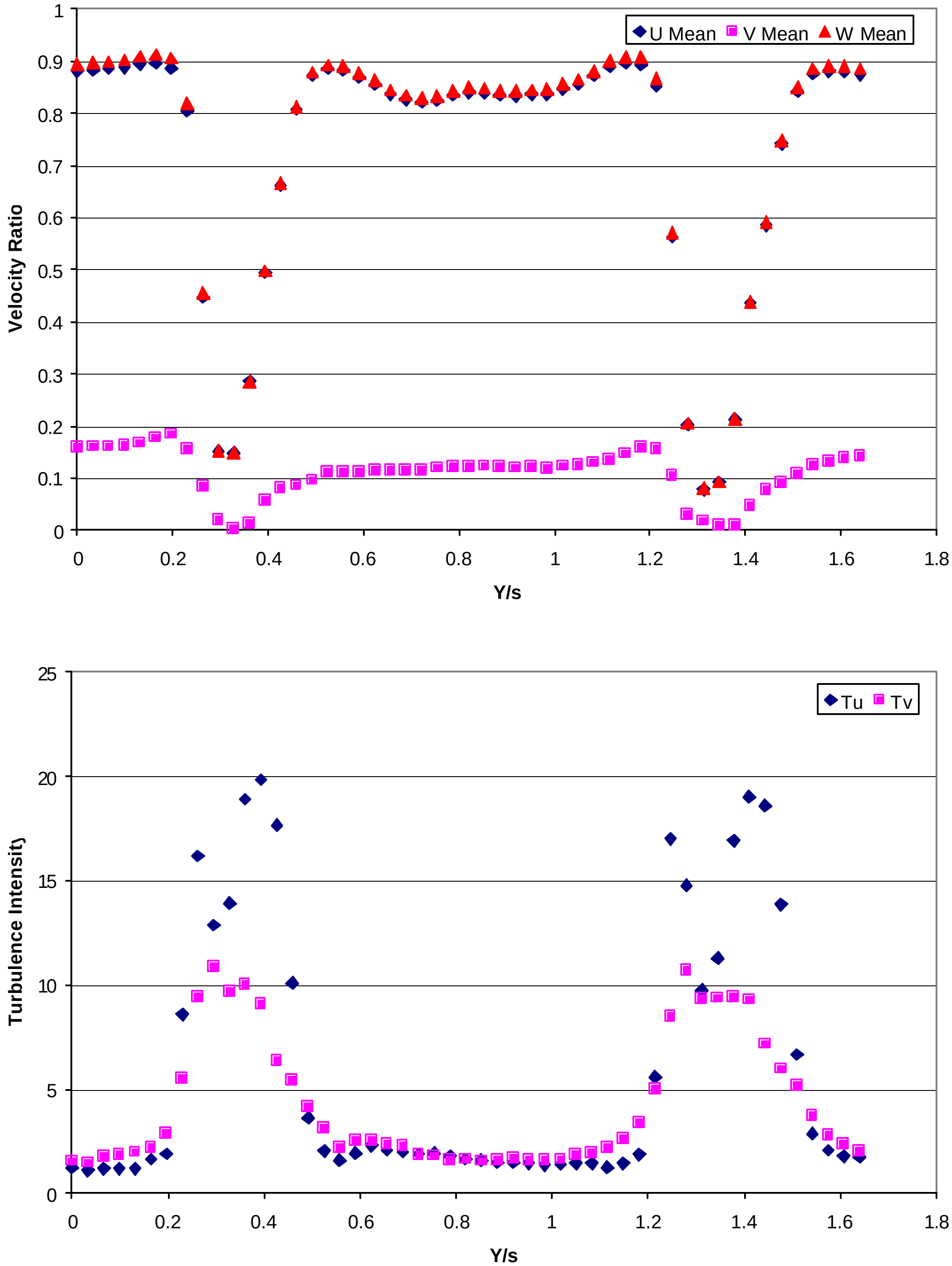

Figure 25. Station 13 Survey

THIS PAGE INTENTIONALLY LEFT BLANK

V. CONCLUSIONS AND RECOMMENDATIONS

A. CONCLUSIONS

A set of second-generation, controlled-diffusion blades in cascade were experimentally examined at stall in a low speed cascade wind tunnel. The experiment was conducted at an off-design inlet flow angle of 40.5 degrees and a Reynolds number of 640,000.

Experimental blade surface pressure measurements were taken at mid span on the blade. When compared to previous recorded data, a decrease in the overall Cp value could be seen across the suction side of the blade. The overall blade loading was decreased and hence the cascade was in stall. Surface-flow visualization using a titanium oxide and kerosene mixture was preformed. The presence of the separation region, in addition to the behavior of the end wall boundary layer, was evident from the visualization. The flow visualization showed the complex three-dimensional nature of the flow separation. Reverse flow was seen at the mid span of the blade, a result of the coalescence of the two corner vortices present. Mid-span LDV data were recorded at the inlet, in the boundary layers and in the wake regions to characterize the flow. The LDV data demonstrated that the separation of the flow occurred between a x/c of 0.61 and 0.68. Reverse flow was recorded after separation had occurred and well into the wake region.

B. RECOMMENDATIONS

Further LDV surveys should be preformed off mid span to accurately determine the span wise line of separation. Three-component LDV surveys should be preformed to map the complex nature of the reverse flow region in addition to the corner vortices. Additional flow visualization with fog should be preformed to determine the flow both at the surface and just off the surface of the blade. The use of fog would remove the influence of the gravity effect that is present in the titanium oxide and kerosene mixture flow visualization.

THIS PAGE INTENTIONALLY LEFT BLANK

APPENDIX A. SURFACE PRESSURE MEASUREMENTS AT VARIOUS REYNOLDS NUMBERS

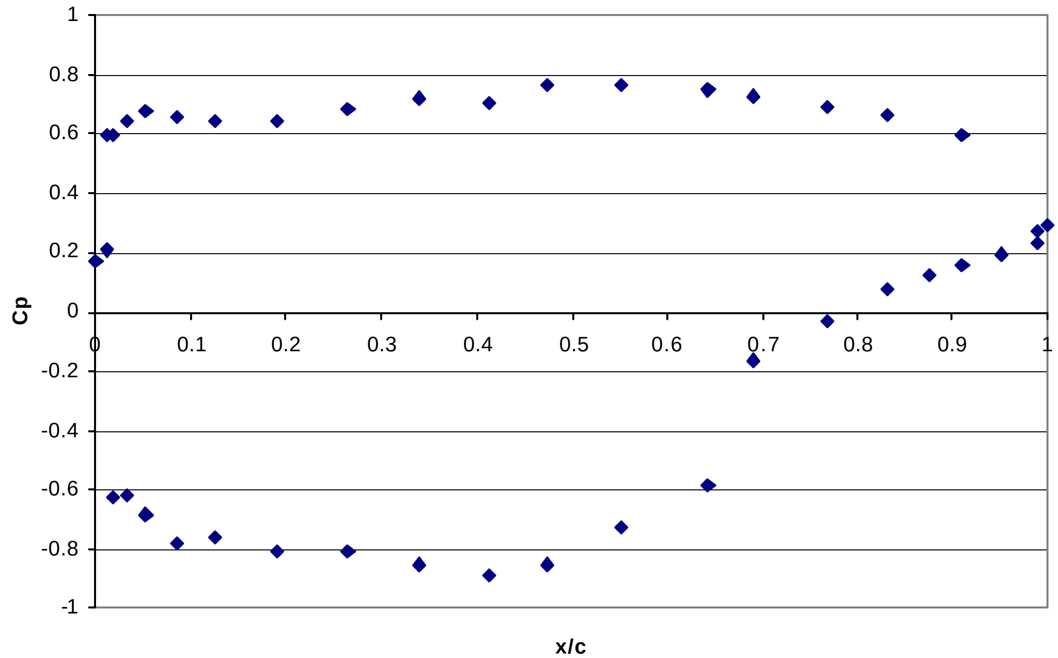

Figure A.1 Reynolds Number of Approximately 290,000

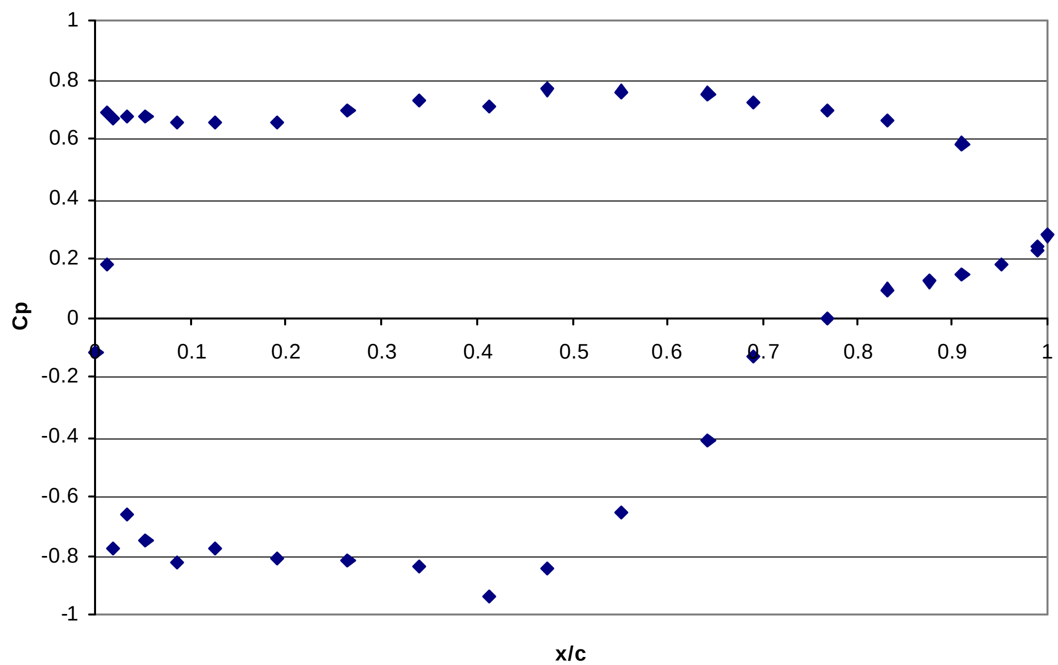

Figure A.2 Reynold Number of Approximately 400,000

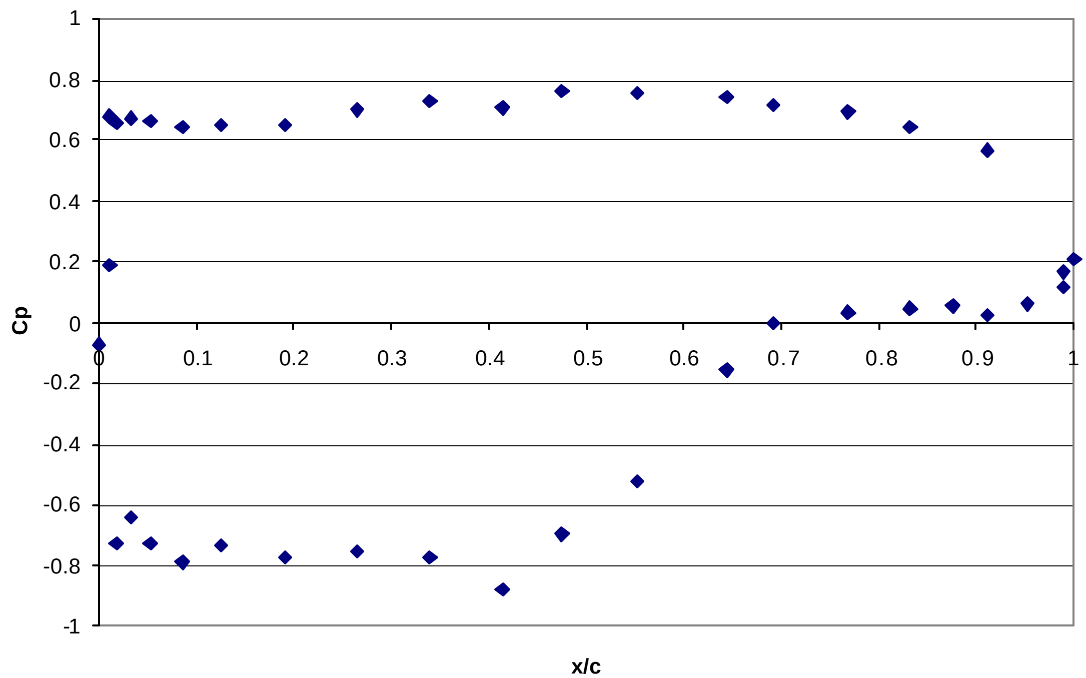

Figure A.3 Reynolds Number of Approximately 490,000

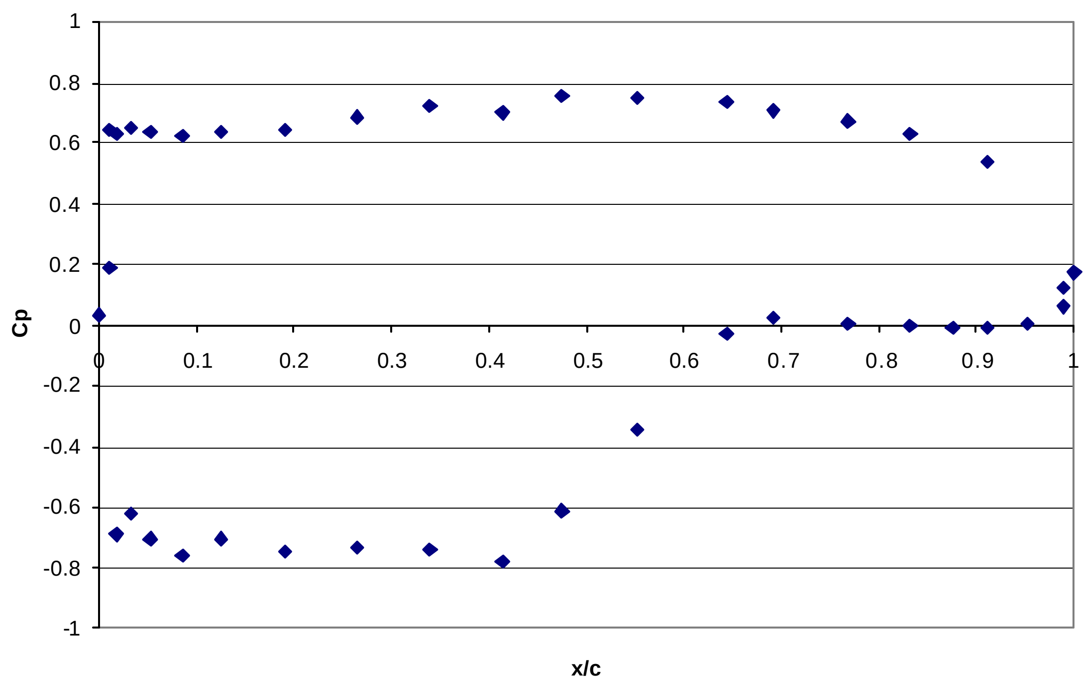

Figure A.4 Reynolds Number of Approximately 590,000

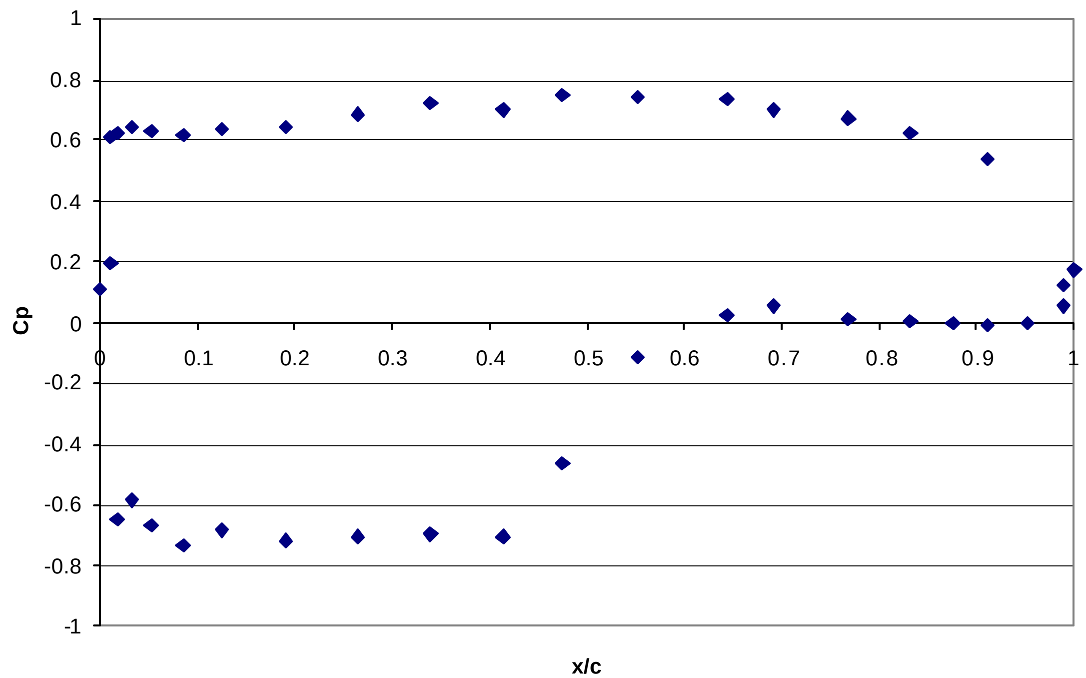

Figure A.5 Reynolds Number of Approximately 670,000

THIS PAGE INTENTIONALLY LEFT BLANK

APPENDIX B. FLOW VISUALIZATION AT VARIOUS REYNOLDS NUMBERS

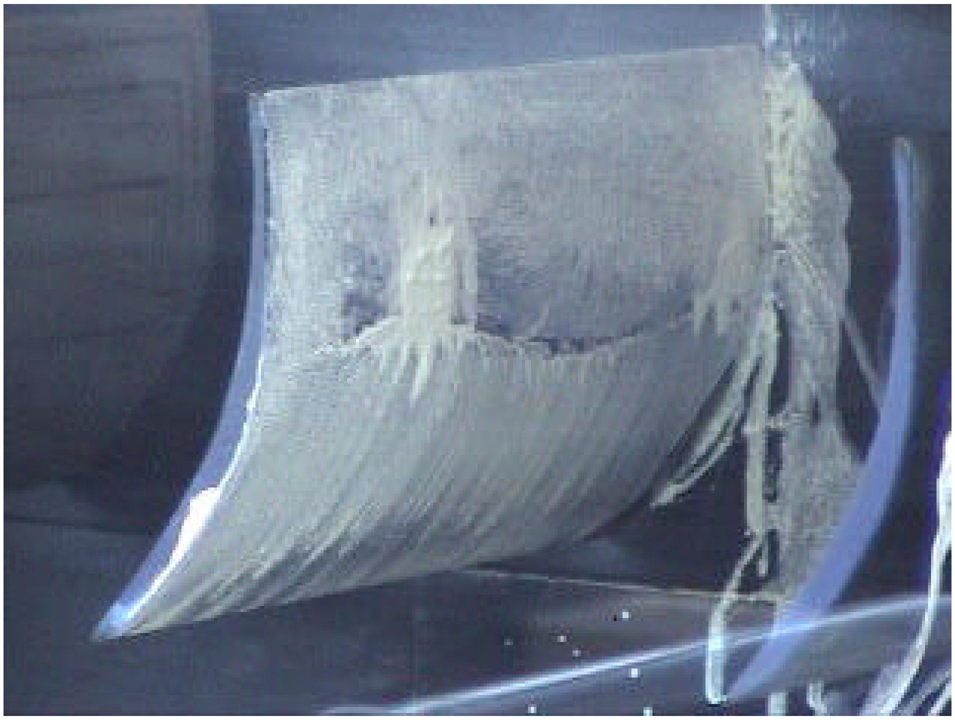

Figure B.1 Reynolds Number of Approximately 290,000

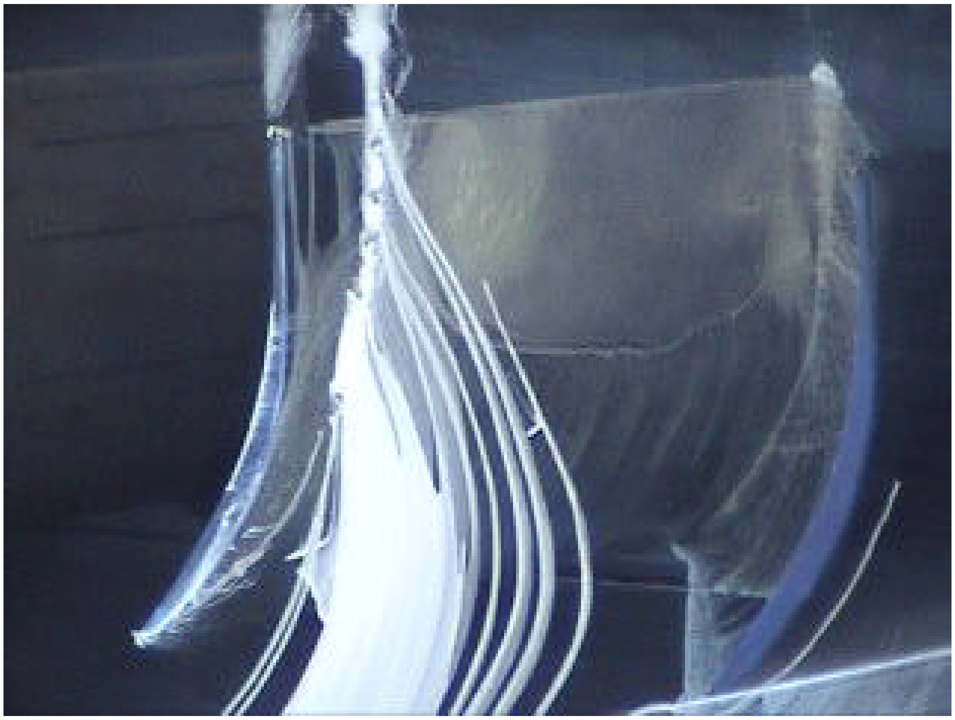

Figure B.2 Reynolds Number of Approximately 550,000

THIS PAGE INTENTIONALLY LEFT BLANK

APPENDIX C. LDV RAW DATA

The inlet flow velocity in the test section, V_{ref} [m/s], was calculated for each survey to allow for the non-dimensionalizing of the data. Each calculation was accomplished using a FORTRAN program titled "CALIB1.FOR" which used the atmospheric pressure, plenum total pressure and plenum total temperature for the respective survey. The details of the program can be found in Reference 3.

Station 1
Feb 23 2004
V_ref 72.1809

x(mm)	y(mm)	y/s	U/V_ref	V/Vref	Tu	Tv	W/V_ref	Re Stress	Corr
-36.576	0	0	0.724171	0.677695	1.496202	2.25164	0.991814	0.126266	0.071937
-36.576	6.349	0.04166	0.729604	0.683002	1.46857	2.455303	0.999407	0.130539	0.069486
-36.576	12.699	0.083327	0.730056	0.669994	1.47399	2.51934	0.990895	0.136895	0.070756
-36.576	19.05	0.125	0.733884	0.66496	1.463416	2.305143	0.990331	0.032236	0.018341
-36.576	25.399	0.16666	0.739856	0.657918	1.406704	2.098837	0.990072	0.04643	0.030184
-36.576	31.75	0.208333	0.749614	0.655442	1.552495	1.902434	0.995752	0.114798	0.074602
-36.576	38.1	0.25	0.764323	0.653976	1.724679	1.95567	1.005918	0.221975	0.126315
-36.576	44.45	0.291667	0.776416	0.649772	1.601171	1.785033	1.012435	0.069863	0.046916
-36.576	50.799	0.333327	0.781293	0.641261	1.381513	1.792376	1.010759	0.049267	0.038188
-36.576	57.149	0.374993	0.782041	0.629622	1.349521	1.923232	1.003998	0.023684	0.017515
-36.576	63.5	0.416667	0.776732	0.622503	1.332313	1.852337	0.9954	0.060904	0.047367
-36.576	69.849	0.458327	0.773112	0.61423	1.421451	1.710238	0.987411	0.129807	0.102486
-36.576	76.2	0.5	0.770892	0.611651	1.578772	1.738941	0.984069	0.083964	0.058701
-36.576	82.549	0.54166	0.767357	0.614201	1.626704	1.778788	0.982894	0.152685	0.101279
-36.576	88.9	0.583333	0.7645	0.615214	1.772256	1.763923	0.9813	0.138275	0.084897
-36.576	95.25	0.625	0.766145	0.619735	1.80293	1.848092	0.985417	0.145995	0.084099
-36.576	101.599	0.66666	0.761747	0.617711	1.542988	1.680982	0.980728	0.142091	0.105147
-36.576	107.95	0.708333	0.752509	0.615829	1.549349	1.837948	0.972376	0.125575	0.08464
-36.576	114.299	0.749993	0.745291	0.621957	1.367058	1.646363	0.970715	0.089782	0.076566
-36.576	120.65	0.791667	0.73662	0.624884	1.555646	1.759505	0.965966	0.072534	0.050862
-36.576	127	0.833333	0.727328	0.631484	1.558002	1.783337	0.963213	0.116247	0.080304
-36.576	133.349	0.874993	0.722319	0.640664	1.50828	1.821625	0.965502	0.053548	0.037407
-36.576	139.699	0.91666	0.718599	0.652306	1.372976	1.988097	0.970509	0.015687	0.01103
-36.576	146.05	0.958333	0.716965	0.662254	1.412006	1.743305	0.976021	0.135334	0.105525
-36.576	152.4	1	0.71901	0.670485	1.531377	2.218105	0.98312	0.13722	0.077538

Station 5bl (U Component)
Mar 18 2004
V_ref 73.2894

x(mm)	y(mm)	y/s	d/c	U/V_ref	Tu
-10.028	23.914	0.156916	0.169403	0.802389	2.35335
-9.278	23.251	0.152566	0.16153	0.808319	2.252243
-8.528	22.589	0.148222	0.153661	0.814433	2.001624
-7.777	21.928	0.143885	0.145792	0.820091	1.669845
-7.027	21.265	0.139534	0.137919	0.819485	1.656852
-6.277	20.603	0.13519	0.130051	0.82352	1.55152
-5.527	19.942	0.130853	0.122188	0.825085	1.583619
-4.777	19.28	0.126509	0.114319	0.82601	1.598264
-4.027	18.617	0.122159	0.106446	0.825148	1.697123
-3.278	17.955	0.117815	0.098583	0.825634	2.057355
-2.528	17.294	0.113478	0.09072	0.82341	2.5708
-1.778	16.632	0.109134	0.082852	0.823653	2.82755
-1.028	15.97	0.10479	0.074984	0.823744	3.250428
-0.278	15.307	0.10044	0.06711	0.815309	4.050177
0.471	14.646	0.096102	0.059253	0.83617	2.569367
1.221	13.983	0.091752	0.05138	0.834867	3.563955
1.971	13.321	0.087408	0.043511	0.825616	5.068886
2.721	12.66	0.083071	0.035648	0.813335	6.188223
3.471	11.997	0.07872	0.027775	0.796872	6.713897
4.222	11.336	0.074383	0.019906	0.769347	7.310838
4.972	10.673	0.070033	0.012033	0.542186	9.930411

Station 5bl (V component)
Mar 23 2004
V_ref 71.7122

x (mm)	y (mm)	y/s	d/c	V/V_ref	Tv
-10.028	23.914	0.156916	0.169403	0.772128	1.548495
-9.278	23.251	0.152566	0.16153	0.78092	1.49611
-8.528	22.589	0.148222	0.153661	0.787743	1.492214
-7.777	21.928	0.143885	0.145792	0.79726	1.563547
-7.027	21.265	0.139534	0.137919	0.807097	1.620691
-6.277	20.603	0.13519	0.130051	0.811061	1.664006
-5.527	19.942	0.130853	0.122188	0.821959	1.611796
-4.777	19.28	0.126509	0.114319	0.834349	1.619054
-4.027	18.617	0.122159	0.106446	0.843788	1.639514
-3.278	17.955	0.117815	0.098583	0.85213	1.621092
-2.528	17.294	0.113478	0.09072	0.865571	1.414802
-1.778	16.632	0.109134	0.082852	0.871882	1.455913
-1.028	15.97	0.10479	0.074984	0.880895	1.22321
-0.278	15.307	0.10044	0.06711	0.88921	1.158561
0.471	14.646	0.096102	0.059253	0.896769	1.288496
1.221	13.983	0.091752	0.05138	0.902841	1.429793
1.971	13.321	0.087408	0.043511	0.892685	4.206715
2.721	12.66	0.083071	0.035648	0.854298	7.135987
3.471	11.997	0.07872	0.027775	0.849578	7.375279
4.222	11.336	0.074383	0.019906	0.845361	8.432696
4.972	10.673	0.070033	0.012033	0.39774	15.78009

Station 6bl (U Component)
Mar 18 2004
V_ref 72.5676

x(mm)	y(mm)	y/s	d/c	U/V_ref	Tu
20.713	45.173	0.296411	0.149668	1.009471	1.617254
21.228	44.316	0.290787	0.141804	1.008734	1.580383
21.742	43.457	0.285151	0.133931	1.020533	1.540759
22.256	42.6	0.279528	0.126071	1.027952	1.431711
22.769	41.741	0.273891	0.118201	1.03683	1.294597
23.283	40.884	0.268268	0.110341	1.041498	1.360196
23.797	40.026	0.262638	0.102475	1.049521	1.384654
24.312	39.167	0.257001	0.094597	1.053739	1.375466
24.826	38.31	0.251378	0.086737	1.060428	1.557175
25.339	37.451	0.245741	0.078867	1.068817	1.650168
25.853	36.594	0.240118	0.071007	1.078906	1.612845
26.367	35.735	0.234482	0.063134	1.086351	1.601629
26.882	34.878	0.228858	0.05527	1.099318	1.660729
27.396	34.02	0.223228	0.047403	1.105278	1.61175
27.91	33.161	0.217592	0.03953	1.114973	1.532675
28.423	32.304	0.211969	0.031674	1.123435	1.52667
28.937	31.446	0.206339	0.023807	1.136252	1.488877
29.452	30.588	0.200709	0.015936	1.122027	3.319932
29.966	29.73	0.195079	0.008069	1.539351	0.524552

Station 6bl (V Component)
Mar 23 3004
V_ref 72.5872

x(mm)	y(mm)	y/s	d/c	U/V_ref	Tu
20.713	45.173	0.296411	0.131996	0.630247	1.614039
21.228	44.316	0.290787	0.124137	0.637017	1.599831
21.742	43.457	0.285151	0.116268	0.642736	1.593619
22.256	42.6	0.279528	0.108414	0.646232	1.47982
22.769	41.741	0.273891	0.100552	0.645173	1.513073
23.283	40.884	0.268268	0.0927	0.648665	1.621443
23.797	40.026	0.262638	0.084843	0.652134	1.590301
24.312	39.167	0.257001	0.076977	0.653559	1.570894
24.826	38.31	0.251378	0.069132	0.65816	1.555529
25.339	37.451	0.245741	0.06128	0.663244	1.590273
25.853	36.594	0.240118	0.053443	0.667384	1.747357
26.367	35.735	0.234482	0.045601	0.671501	1.661408
26.882	34.878	0.228858	0.037783	0.678496	1.6955
27.396	34.02	0.223228	0.029984	0.681699	1.851146
27.91	33.161	0.217592	0.022226	0.701241	2.397353
28.423	32.304	0.211969	0.014609	0.700212	1.675956
28.937	31.446	0.206339	0.007495	0.700083	1.430831
29.452	30.588	0.200709	0.004773	0.68873	2.139127
29.966	29.73	0.195079	0.010637	0.338645	6.430227

Station 7 bl
Mar 9 2004
V_ref 71.5698

x(mm)	y(mm)	y/s	d/c	U/V_ref	Tu
56.909	67.149	0.44061	0.212749	0.967741	1.785636
57.059	66.159	0.434114	0.204873	0.976007	1.663135
57.209	65.169	0.427618	0.196998	0.979306	1.74001
57.359	64.179	0.421122	0.189122	0.986028	1.68733
57.509	63.189	0.414626	0.181247	0.990061	1.48334
57.659	62.199	0.40813	0.173371	0.99342	1.855461
57.809	61.209	0.401634	0.165496	0.999085	1.59358
57.959	60.219	0.395138	0.157621	1.004446	1.621718
58.109	59.229	0.388642	0.149745	1.006053	1.756105
58.259	58.239	0.382146	0.14187	1.011509	1.568759
58.409	57.249	0.37565	0.133994	1.017245	1.837378
58.559	56.259	0.369154	0.126119	1.021357	1.745489
58.709	55.269	0.362657	0.118244	1.019806	1.923323
58.859	54.279	0.356161	0.110368	1.024456	1.744853
58.259	58.239	0.382146	0.14187	1.00186	1.736113
58.409	57.249	0.37565	0.133994	1.004689	1.668146
58.559	56.259	0.369154	0.126119	1.007637	1.709316
58.709	55.269	0.362657	0.118244	1.014847	1.718999
58.859	54.279	0.356161	0.110368	1.017579	1.641782
59.009	53.289	0.349665	0.102493	1.021956	1.702303
59.159	52.299	0.343169	0.094618	1.025998	1.804362
59.309	51.309	0.336673	0.086743	1.025787	1.484027
59.459	50.319	0.330177	0.078868	1.028263	1.638743
59.609	49.329	0.323681	0.070993	1.033757	1.739555
59.759	48.339	0.317185	0.063118	1.032994	1.759251
59.909	47.349	0.310689	0.055243	1.035304	1.513904
60.059	46.359	0.304193	0.047369	1.032433	1.539244
60.209	45.369	0.297697	0.039495	1.03541	1.509297
60.509	43.389	0.284705	0.023751	0.932969	8.664986
60.659	42.399	0.278209	0.015884	0.6044	12.94921
60.959	40.419	0.265217	0.000925	0.492319	3.409755
60.059	46.359	0.304193	0.047369	1.049258	2.109156
60.209	45.369	0.297697	0.039495	1.052357	2.277375
60.509	43.389	0.284705	0.023751	0.971943	7.773633
60.659	42.399	0.278209	0.015884	0.621208	11.54253
60.809	41.409	0.271713	0.008035	0.544663	5.252286
60.959	40.419	0.265217	0.000925	0.462873	2.56E-07

Station 7.25bl - 1
Mar 16 2004
V_ref 71.7951

x(mm)	y(mm)	y/s	d/c	U/V_ref	Tu
67.591	60.764	0.398714	0.153566	0.987735	1.798526
67.641	59.764	0.392152	0.145692	0.990244	1.765774
67.691	58.764	0.385591	0.137818	0.98366	1.841216
67.742	57.764	0.379029	0.129944	0.989378	2.001443
67.792	56.764	0.372467	0.12207	0.992246	2.095088
67.841	55.764	0.365906	0.114197	0.991089	1.903197
67.891	54.764	0.359344	0.106324	0.996906	1.916503
67.941	53.764	0.352782	0.098451	0.996007	1.793549
67.992	52.764	0.34622	0.090578	0.997557	2.016282
68.042	51.764	0.339659	0.082706	0.995359	1.920436
68.091	50.764	0.333097	0.074835	0.994718	1.763128
68.141	49.764	0.326535	0.066964	0.99698	1.913285
68.191	48.764	0.319974	0.059095	0.994493	2.094799
68.242	47.764	0.313412	0.051227	0.99376	1.986347
68.292	46.764	0.30685	0.043362	0.965953	5.366778
68.341	45.764	0.300289	0.035502	0.718286	15.34201
68.391	44.764	0.293727	0.027651	0.487228	13.7945
68.441	43.764	0.287165	0.019818	0.308599	11.92353
68.492	42.764	0.280604	0.012038	0.174112	5.130859
68.492	42.764	0.280604	0.012038	0	0

Station 7.25bl - 2
Mar 16 2004
V_ref 72.0247

x(mm)	y(mm)	y/s	d/c	U/V_ref	Tu
68.266	47.264	0.310131	0.047295	0.607247	18.81774
68.292	46.764	0.30685	0.043362	0.624493	17.10754
68.316	46.264	0.30357	0.039432	0.509127	13.25679
68.341	45.764	0.300289	0.035502	0.53692	10.89663
68.367	45.264	0.297008	0.031574	0.489857	11.74667
68.391	44.764	0.293727	0.027651	0.433773	12.93265
68.417	44.264	0.290446	0.02373	0.348789	12.92206
68.441	43.764	0.287165	0.019818	0.252559	13.04829
68.466	43.264	0.283885	0.015917	0.129072	12.77827
68.492	42.764	0.280604	0.012038	-0.02026	6.643603
68.516	42.264	0.277323	0.008221	0.315453	4.490377
68.542	41.764	0.274042	0.004602	0.326631	3.827429

Station 7.5 - 1
Mar 15 2004
V_ref 71.4243

x(mm)	y(mm)	y/s	d/c	U/V_ref	Tu
76.257	70.34	0.461549	0.228326	0.949786	1.703384
76.256	69.34	0.454987	0.22046	0.953164	1.692496
76.254	68.34	0.448425	0.212595	0.951749	1.724598
76.251	67.34	0.441864	0.20473	0.956422	1.756125
76.25	66.34	0.435302	0.196864	0.963417	1.674525
76.248	65.34	0.42874	0.188999	0.960436	1.692366
76.245	64.34	0.422178	0.181134	0.961552	1.766285
76.243	63.34	0.415617	0.173268	0.963763	1.770105
76.242	62.34	0.409055	0.165403	0.968712	1.864025
76.239	61.34	0.402493	0.157538	0.969566	1.826818
76.237	60.34	0.395932	0.149673	0.972444	1.831121
76.236	59.34	0.38937	0.141807	0.976276	1.809
76.233	58.34	0.382808	0.133942	0.981132	1.761663
76.231	57.34	0.376247	0.126077	0.980035	1.842671
76.23	56.34	0.369685	0.118211	0.980143	1.699087
76.227	55.34	0.363123	0.110346	0.98158	1.718757
76.225	54.34	0.356562	0.102481	0.980672	1.890784
76.224	53.34	0.35	0.094616	0.980897	2.036608
76.221	52.34	0.343438	0.086751	0.985264	2.132988
76.219	51.34	0.336877	0.078885	0.982064	2.214072
76.218	50.34	0.330315	0.07102	0.979242	2.713011
76.215	49.34	0.323753	0.063155	0.931126	8.659469
76.213	48.34	0.317192	0.05529	0.747849	17.2187
76.212	47.34	0.31063	0.047426	0.575881	15.00343
76.209	46.34	0.304068	0.039561	0.403364	13.25047
76.207	45.34	0.297507	0.031697	0.276811	11.25368
76.206	44.34	0.290945	0.023834	0.175685	5.30473
76.203	43.34	0.284383	0.015972	0.316096	18.23928
76.201	42.34	0.277822	0.008119	0.472476	6.3129
76.2	41.34	0.27126	0.000677	0	0

Station 7.5bl - 2
Mar 16 2004
V_ref 71.9273

x(mm)	y(mm)	y/s	d/c	U/V_ref	Tu
76.212	48.34	0.317192	0.05529	0.451817	14.08003
76.212	47.84	0.313911	0.051358	0.436121	13.99041
76.21	47.34	0.31063	0.047426	0.416117	14.95763
76.209	46.84	0.307349	0.043493	0.371546	14.77724
76.209	46.34	0.304068	0.039561	0.288062	15.18442
76.207	45.84	0.300787	0.035629	0.203817	15.53048
76.206	45.34	0.297507	0.031697	0.122133	13.93118
76.206	44.84	0.294226	0.027765	0.025878	10.62034
76.204	44.34	0.290945	0.023834	-0.038725	5.817102
76.203	43.84	0.287664	0.019902	-0.072083	2.98658
76.203	43.34	0.284383	0.015972	-0.078095	2.440711
76.201	42.84	0.281102	0.012043	-0.071829	2.414871
76.2	42.34	0.277822	0.008118	-0.002435	1.429658
76.2	41.84	0.274541	0.004209	0.327909	4.484744
76.198	41.34	0.27126	0.000662	0	0

Station 8bl - 1
Mar 8 2004
V_ref 72.6541

x(mm)	y(mm)	y/s	d/c	U/V_ref	Tu
93.748	75.686	0.496627	0.275406	0.936291	1.770929
93.683	74.688	0.490079	0.26754	0.942756	1.848019
93.617	73.691	0.483537	0.259681	0.941985	1.716335
93.551	72.692	0.476982	0.251807	0.94479	1.723997
93.484	71.694	0.470433	0.24394	0.948629	1.782692
93.418	70.697	0.463891	0.236081	0.949361	1.736211
93.352	69.698	0.457336	0.228206	0.952582	1.722145
93.287	68.7	0.450787	0.22034	0.956364	1.816959
93.221	67.703	0.444245	0.212481	0.957594	1.790604
93.155	66.704	0.43769	0.204607	0.961635	2.084324
93.088	65.706	0.431142	0.19674	0.963958	1.884557
93.022	64.709	0.4246	0.188881	0.964506	2.169366
92.956	63.71	0.418045	0.181007	0.967184	1.96498
92.891	62.713	0.411503	0.173149	0.966847	2.185471
92.825	61.715	0.404954	0.165282	0.969062	2.484054
92.759	60.716	0.398399	0.157408	0.970566	2.615685
92.692	59.719	0.391857	0.149549	0.972326	2.872427
92.626	58.72	0.385302	0.141674	0.972057	3.00279
92.561	57.722	0.378753	0.133809	0.968592	3.969562
92.495	56.725	0.372211	0.12595	0.941147	6.870365
92.429	55.726	0.365656	0.118076	0.834982	15.53134
92.099	50.737	0.33292	0.078754	0.211075	16.38554
92.033	49.738	0.326365	0.070881	0.136535	14.92657
91.966	48.74	0.319816	0.063015	0.058734	12.69334
91.9	47.743	0.313274	0.055158	-0.030634	6.307086
91.834	46.744	0.306719	0.047286	-0.062141	3.703785
91.769	45.746	0.300171	0.039424	-0.071657	3.154848
91.703	44.749	0.293629	0.031571	-0.077988	2.776492
91.637	43.75	0.287073	0.023707	-0.07737	2.478669
91.57	42.753	0.280531	0.015867	-0.079026	2.474395

Station 8bl - 2
Mar 8 2004
V_ref 72.8992

x(mm)	y(mm)	y/s	d/c	U/V_ref	Tu
60.716	92.759	0.398399	0.157408	0.980795	2.227092
59.719	92.692	0.391857	0.149549	0.981012	2.411926
58.72	92.626	0.385302	0.141674	0.976337	3.024566
57.722	92.561	0.378753	0.133809	0.973119	3.793763
56.725	92.495	0.372211	0.12595	0.948065	6.684875
55.726	92.429	0.365656	0.118076	0.785428	18.74205
54.728	92.362	0.359108	0.110209	0.668756	18.56869
53.731	92.296	0.352566	0.102351	0.589057	17.21885
52.732	92.23	0.34601	0.094477	0.534804	15.15314
51.734	92.165	0.339462	0.086612	0.450282	13.43056
50.737	92.099	0.33292	0.078754	0.374431	13.86802

Station 9bl
Mar 8 2004
V_ref 71.6203

x(mm)	y(mm)	y/s	d/c	U/V_ref	Tu
119.021	80.001	0.524941	0.322907	0.937744	2.00891
118.943	79.003	0.518392	0.315034	0.939304	2.191188
118.865	78.005	0.511844	0.30716	0.944845	1.950123
118.787	77.007	0.505295	0.299287	0.949065	2.127832
118.709	76.009	0.498747	0.291413	0.94903	2.231966
118.631	75.011	0.492198	0.28354	0.951899	2.543474
118.553	74.013	0.48565	0.275666	0.95616	2.283837
118.475	73.015	0.479101	0.267793	0.958154	3.161804
118.397	72.017	0.472552	0.259919	0.963725	2.748535
118.319	71.019	0.466004	0.252046	0.960961	3.24552
118.241	70.021	0.459455	0.244172	0.966409	3.592219
118.163	69.023	0.452907	0.236299	0.965395	4.706968
118.085	68.025	0.446358	0.228425	0.960168	5.119835
118.007	67.027	0.43981	0.220552	0.961877	5.309781
117.929	66.029	0.433261	0.212678	0.954122	6.316993
117.851	65.031	0.426713	0.204805	0.923325	8.987468
117.773	64.033	0.420164	0.196931	0.900777	11.66046
117.695	63.035	0.413615	0.189058	0.880394	13.23356
117.617	62.037	0.407067	0.181184	0.793212	17.15591
117.539	61.039	0.400518	0.173311	0.736555	19.00084
117.461	60.041	0.39397	0.165438	0.67366	20.54554
117.383	59.043	0.387421	0.157564	0.642552	21.79621
117.305	58.045	0.380873	0.149691	0.575341	19.43249
117.227	57.047	0.374324	0.141817	0.485957	19.92313
117.149	56.048	0.367769	0.133936	0.314609	18.4304
117.07	55.051	0.361227	0.12607	0.258989	18.01012
116.992	54.052	0.354672	0.118189	0.195428	17.07469
116.915	53.054	0.348123	0.110316	0.147528	15.44367
116.837	52.057	0.341581	0.102451	0.096043	14.03298
116.759	51.058	0.335026	0.09457	0.047651	12.22781
116.68	50.06	0.328478	0.086696	0.014089	9.968406
116.602	49.063	0.321936	0.078831	-0.021906	7.014873
116.525	48.064	0.315381	0.070951	-0.035769	6.044038
116.447	47.067	0.308839	0.063086	-0.045313	5.101021
116.368	46.069	0.30229	0.055213	-0.060225	4.385279
116.29	45.07	0.295735	0.047333	-0.062745	3.959402
116.212	44.073	0.289193	0.039469	-0.069209	3.732198
116.135	43.075	0.282644	0.031599	-0.077644	3.113267
116.057	42.076	0.276089	0.023722	-0.078811	3.124585
115.978	41.079	0.269547	0.015865	-0.081173	2.985773
115.9	40.081	0.262999	0.008019	0.322953	4.742373
115.822	39.082	0.256444	0.000949	0	0

Station 11
Feb 24 2004
V_ref 72.1196

x(mm)	y(mm)	y/s	U/V_ref	V/V_ref	Tu	Tv	W/V_ref	Re Stress	Corr
128.014	0	0	0.868695	0.14731	1.339233	1.720424	0.881097	0.097627	0.081327
128.014	2.5	0.016404	0.868746	0.143398	1.235201	1.583975	0.880502	0.09544	0.093627
128.014	5	0.032808	0.869916	0.137708	1.492741	1.872521	0.880748	0.085321	0.058587
128.014	7.5	0.049213	0.872746	0.132785	1.50149	1.873151	0.882789	0.117631	0.080275
128.014	10	0.065617	0.872862	0.125201	1.282602	2.009357	0.881796	0.060437	0.04501
128.014	12.5	0.082021	0.876945	0.118329	1.286023	2.106549	0.884893	0.127357	0.090231
128.014	15	0.098425	0.880201	0.110723	1.41972	2.077316	0.887138	0.115181	0.07496
128.014	17.5	0.114829	0.884669	0.100675	1.36132	2.014785	0.89038	0.118703	0.083067
128.014	20	0.131234	0.8929	0.091226	1.06672	1.917998	0.897548	0.07622	0.071503
128.014	22.5	0.147638	0.92581	0.084484	1.494785	2.001073	0.929657	0.041289	0.026494
128.014	25	0.164042	0.944045	0.077476	1.604791	1.985946	0.947219	0.036281	0.02185
128.014	27.5	0.180446	0.964396	0.066933	1.756812	2.037292	0.966716	0.160346	0.085987
128.014	30	0.19685	0.991718	0.059779	1.722049	2.056235	0.993518	0.161283	0.087423
128.014	32.5	0.213255	1.005519	0.059561	3.025065	2.610751	1.007282	0.298771	0.07261
128.014	35	0.229659	0.413334	0.047786	15.42561	9.271703	0.416087	6.34179	0.085107
128.014	38.5	0.252625	-0.091008	-0.113205	6.088927	6.308716	0.14525	-1.44238	-0.07207
128.014	40	0.262467	-0.100516	-0.109995	5.659016	6.47216	0.149005	-0.119654	-0.00627
128.014	42.5	0.278871	-0.092661	-0.109286	6.442205	6.626352	0.14328	-1.3611	-0.061198
128.014	45	0.295276	-0.077905	-0.105424	7.242078	6.679006	0.131085	-0.717135	-0.028457
128.014	47.5	0.31168	-0.060593	-0.103098	8.598779	6.872165	0.119586	-2.14928	-0.06981
128.014	50	0.328084	-0.018304	-0.121238	11.15702	7.838812	0.122612	-6.53042	-0.143317
128.014	52.5	0.344488	0.023364	-0.123846	12.00918	7.934805	0.126031	-1.11533	-0.022465
128.014	55	0.360892	0.076549	-0.121938	11.61244	7.130825	0.143974	-2.69201	-0.062398
128.014	57.5	0.377297	0.100864	-0.115544	10.74821	7.072365	0.153376	0.219797	0.00555
128.014	60	0.393701	0.54908	0.084439	18.97885	7.671529	0.555535	-3.60828	-0.047567
128.014	62.5	0.410105	0.650144	0.11142	17.58387	6.061488	0.659622	1.80778	0.032554
128.014	65	0.426509	0.726496	0.124366	15.35092	5.886286	0.737063	2.04457	0.043429
128.014	67.5	0.442913	0.809016	0.139882	10.68395	4.867484	0.821019	1.09204	0.040305
128.014	70	0.459318	0.867362	0.15403	5.041119	3.917098	0.880934	0.435581	0.042338
128.014	72.5	0.475722	0.885374	0.161119	2.953705	3.041375	0.899914	-0.172437	-0.036843
128.014	75	0.492126	0.895048	0.164866	1.901047	2.637746	0.910105	-0.064566	-0.024713
128.014	77.5	0.50853	0.900051	0.165598	1.476777	2.299127	0.915158	-0.048235	-0.027267
128.014	80	0.524934	0.900435	0.16627	1.112514	1.948366	0.915658	0.073213	0.064828
128.014	82.5	0.541339	0.898702	0.167512	1.372336	2.09605	0.914181	0.099159	0.066165
128.014	85	0.557743	0.894814	0.168567	1.210031	2.020053	0.910553	0.133514	0.10484
128.014	87.5	0.574147	0.892052	0.164246	1.25947	1.913363	0.907046	0.152287	0.121292
128.014	90	0.590551	0.885017	0.16453	1.348518	1.985742	0.90018	0.178467	0.127919
128.014	92.5	0.606955	0.878005	0.162977	1.514102	2.134831	0.893004	0.303453	0.180188
128.014	95	0.62336	0.871526	0.161694	1.714055	2.228576	0.886398	0.505046	0.253767
128.014	97.5	0.639764	0.862371	0.161381	1.719878	2.183432	0.877342	0.426653	0.218069
128.014	100	0.656168	0.854697	0.157202	1.832334	2.18563	0.869035	0.524324	0.251289

Station 12
Feb 22 2004
V_ref 71.5698

x(mm)	y(mm)	y/s	U/V_ref	V/V_ref	Tu	Tv	W/V_ref	Re Stress	Corr
134.111	0	0	0.878995	0.15168	1.258132	1.525581	0.891987	0.045683	0.046465
134.111	5	0.032808	0.882582	0.1466	1.34689	1.748449	0.894673	0.037901	0.03142
134.111	10	0.065617	0.88551	0.138617	1.378332	1.801841	0.896294	0.060992	0.047945
134.111	15	0.098425	0.895339	0.132885	1.171837	1.92265	0.905147	0.056592	0.049037
134.111	20	0.131234	0.903786	0.127215	1.061994	1.997305	0.912695	-0.009799	-0.009019
134.111	25	0.164042	-0.063376	0.120168	1.393854	2.320038	0.135856	0.063424	0.03829
134.111	30	0.19685	-0.039529	0.123184	1.837705	3.029602	0.129371	-0.055381	-0.01942
134.111	35	0.229659	-0.170645	0.111938	8.095073	7.734573	0.204083	2.48311	0.077424
134.111	40	0.262467	-0.101462	-0.008097	7.745472	8.768779	0.101784	-0.584979	-0.016815
134.111	45	0.295276	-0.097188	-0.008173	8.758889	8.027686	0.097531	0.264631	0.007348
134.111	50	0.328084	-0.143148	0.003724	10.1537	5.138328	0.143197	-2.79681	-0.104654
134.111	55	0.360892	0.351457	0.173668	16.86937	11.71074	0.392024	5.00823	0.049493
134.111	60	0.393701	0.579275	0.195278	18.94299	10.96433	0.611304	2.29872	0.021607
134.111	65	0.426509	0.749021	0.192256	14.42383	10.18488	0.773302	-6.83739	-0.090864
134.111	70	0.459318	0.885664	0.156608	3.32295	5.689348	0.899403	-0.730066	-0.07539
134.111	75	0.492126	0.903855	0.144812	1.601983	3.04057	0.915382	-0.085687	-0.034343
134.111	80	0.524934	0.904931	0.144811	1.277997	2.180261	0.916445	0.091275	0.063952
134.111	85	0.557743	0.898108	0.150508	1.199396	1.816476	0.910631	0.120676	0.108135
134.111	90	0.590551	0.884391	0.145288	1.708193	2.304638	0.896245	0.287518	0.142583
134.111	95	0.62336	0.867798	0.139988	1.974812	2.363652	0.879016	0.389873	0.163062
134.111	100	0.656168	0.84567	0.136598	2.081548	2.247472	0.856631	0.408622	0.170523
134.111	105	0.688976	0.832892	0.133835	1.918375	2.010714	0.843576	0.168047	0.085053
134.111	110	0.721785	0.828088	0.132798	1.707675	1.737725	0.838669	0.234842	0.1545
134.111	115	0.754593	0.830388	0.134088	1.837092	1.761303	0.841144	0.299534	0.180726
134.111	120	0.787402	0.836452	0.131901	1.621119	1.612764	0.846787	0.221205	0.165178
134.111	125	0.82021	0.837691	0.129318	1.733527	1.606255	0.847614	0.199106	0.139598
134.111	130	0.853018	0.836323	0.127856	1.545693	1.493398	0.84604	0.157599	0.133289
134.111	135	0.885827	0.833581	0.12645	1.503471	1.560562	0.843117	0.118936	0.098964
134.111	140	0.918635	0.830693	0.123443	1.48954	1.63924	0.839815	0.093304	0.074601
134.111	145	0.951444	0.8313	0.115528	1.45283	1.595352	0.83929	0.111946	0.094293
134.111	150	0.984252	0.838724	0.114336	1.656933	1.554083	0.846481	0.052095	0.039497
134.111	155	1.01706	0.848368	0.111316	1.410309	1.592669	0.855639	0.067033	0.058262
134.111	160	1.049869	0.860659	0.106488	1.600628	1.758717	0.867222	0.027024	0.018741
134.111	165	1.082677	0.876558	0.103152	1.373952	1.848178	0.882607	0.176274	0.135523
134.111	170	1.115486	0.896145	0.100193	1.19517	1.997091	0.90173	0.010153	0.008304
134.111	175	1.148294	0.908334	0.095934	1.188673	2.164633	0.913387	0.031517	0.023913
134.111	180	1.181102	-0.054611	0.086974	1.541469	2.603758	0.102698	0.174216	0.084741
134.111	185	1.213911	-0.052886	0.113359	3.63132	4.247914	0.125089	0.321143	0.040644
134.111	190	1.246719	-0.148532	-0.008997	9.014328	9.359955	0.148804	-1.17295	-0.02714
134.111	195	1.279528	-0.085316	-0.01154	7.930085	7.584147	0.086093	4.1121	0.133481
134.111	200	1.312336	-0.130081	-0.003825	8.639862	4.136859	0.130137	-1.69579	-0.092627
134.111	205	1.345144	-0.122361	0.028355	9.623992	4.610933	0.125604	-3.7101	-0.163223
134.111	210	1.377953	0.306288	0.158234	16.96185	11.7007	0.344747	2.12573	0.020911
134.111	215	1.410761	0.499792	0.197164	18.5991	11.78172	0.537277	2.72561	0.024283
134.111	220	1.44357	0.665877	0.199696	17.13082	10.43621	0.695177	-1.08011	-0.011795
134.111	225	1.476378	0.819983	0.194769	9.616347	8.335289	0.842797	-2.87505	-0.070025
134.111	230	1.509186	0.890167	0.165786	2.177243	3.654728	0.905474	-0.276269	-0.067782
134.111	235	1.541995	0.893775	0.157526	1.624686	2.32272	0.90755	0.120738	0.062462
134.111	240	1.574803	0.888791	0.160625	1.48229	1.982562	0.903188	0.032544	0.02162
134.111	245	1.607612	0.882142	0.158906	1.598846	1.815474	0.89634	0.072153	0.048528
134.111	250	1.64042	0.876252	0.159066	1.602245	1.658896	0.890573	0.160158	0.117635

Station 13
Feb 20 2004
V_ref 71.8583

x(mm)	y(mm)	y/s	U/V_ref	V/V_ref	Tu	Tv	W/V_ref	Re Stress	Corr
146.304	0	0	0.880576	0.160335	1.244483	1.553239	0.895055	0.039428	0.039502
146.304	5	0.032808	0.884005	0.161422	1.095795	1.460503	0.898621	0.062246	0.075322
146.304	10	0.065617	0.885514	0.160464	1.196161	1.785841	0.899935	0.166419	0.150875
146.304	15	0.098425	0.888549	0.16167	1.177407	1.867219	0.903137	0.14615	0.128742
146.304	20	0.131234	0.894126	0.167872	1.197334	1.969576	0.909749	-0.001183	-0.000972
146.304	25	0.164042	0.895773	0.177577	1.635869	2.205758	0.913204	0.018202	0.009769
146.304	30	0.19685	0.887161	0.184702	1.896635	2.895487	0.906185	0.03894	0.013732
146.304	35	0.229659	0.804858	0.154906	8.584692	5.511967	0.819628	1.11616	0.045682
146.304	40	0.262467	0.44648	0.084404	16.17071	9.396885	0.454389	3.84311	0.04898
146.304	45	0.295276	0.151852	0.01967	12.86141	10.89802	0.153119	8.07427	0.111562
146.304	50	0.328084	0.148691	0.002374	13.93479	9.701771	0.148709	0.813157	0.011649
146.304	55	0.360892	0.285808	0.013574	18.89745	10.02458	0.286131	2.50476	0.025606
146.304	60	0.393701	0.494614	0.056726	19.84331	9.099816	0.497856	10.473	0.112324
146.304	65	0.426509	0.661887	0.080576	17.6432	6.364157	0.666775	1.3966	0.024088
146.304	70	0.459318	0.807955	0.085498	10.07787	5.441724	0.812466	0.067622	0.002388
146.304	75	0.492126	0.87337	0.096108	3.637849	4.165614	0.878642	-0.101239	-0.012938
146.304	80	0.524934	0.885765	0.11115	2.033035	3.139528	0.892711	0.10004	0.030354
146.304	85	0.557743	0.883223	0.111777	1.561026	2.222374	0.890267	0.041201	0.023
146.304	90	0.590551	0.870485	0.111696	1.927107	2.536677	0.877622	0.271438	0.107534
146.304	95	0.62336	0.855381	0.114773	2.281736	2.525376	0.863047	0.485552	0.163189
146.304	100	0.656168	0.836918	0.115615	2.056399	2.355128	0.844866	0.430729	0.172237
146.304	105	0.688976	0.826596	0.116237	1.988113	2.285247	0.834729	0.389639	0.166087
146.304	110	0.721785	0.822227	0.115331	1.891236	1.835174	0.830276	0.074822	0.04175
146.304	115	0.754593	0.823876	0.119626	1.91149	1.79616	0.832516	0.288746	0.162871
146.304	120	0.787402	0.835487	0.122595	1.769136	1.612708	0.844434	0.130162	0.088351
146.304	125	0.82021	0.840055	0.12217	1.652682	1.647601	0.848893	0.197582	0.140525
146.304	130	0.853018	0.839531	0.122882	1.57371	1.555193	0.848477	0.139598	0.110462
146.304	135	0.885827	0.835241	0.120866	1.466374	1.606106	0.84394	0.154448	0.127002
146.304	140	0.918635	0.83334	0.119809	1.453737	1.690255	0.84191	0.162014	0.127691
146.304	145	0.951444	0.836595	0.121038	1.440056	1.613081	0.845305	0.136751	0.11401
146.304	150	0.984252	0.837301	0.119129	1.367203	1.624886	0.845733	0.145078	0.126471
146.304	155	1.01706	0.847151	0.123375	1.421231	1.637396	0.856088	0.08502	0.070753
146.304	160	1.049869	0.855731	0.125625	1.442541	1.848038	0.864902	0.062973	0.045747
146.304	165	1.082677	0.872043	0.130313	1.439472	1.950644	0.881726	0.102313	0.070566
146.304	170	1.115486	0.890381	0.136175	1.244157	2.201608	0.900734	0.08953	0.0633
146.304	175	1.148294	0.897131	0.146999	1.444067	2.610732	0.909093	0.124777	0.064097
146.304	180	1.181102	0.893863	0.158765	1.879258	3.375254	0.907853	0.016664	0.005088
146.304	185	1.213911	0.852248	0.156008	5.575697	4.990912	0.866409	0.258881	0.018016
146.304	190	1.246719	0.562454	0.10441	17.02627	8.489069	0.572063	2.7016	0.036198
146.304	195	1.279528	0.203218	0.029145	14.77529	10.67701	0.205298	7.05942	0.086662
146.304	200	1.312336	0.077937	0.017159	9.760708	9.365173	0.079804	-0.521204	-0.011042
146.304	205	1.345144	0.092336	0.009224	11.27628	9.383163	0.092796	-1.11059	-0.020328
146.304	210	1.377953	0.213761	0.010063	16.94287	9.390167	0.213999	2.00417	0.024396
146.304	215	1.410761	0.436341	0.046453	19.00923	9.289233	0.438807	6.46119	0.070862
146.304	220	1.44357	0.585735	0.078297	18.58243	7.1773	0.590945	2.21923	0.032224
146.304	225	1.476378	0.741337	0.091962	13.87123	5.972028	0.747019	-2.33296	-0.05454
146.304	230	1.509186	0.842945	0.108345	6.654133	5.176464	0.84988	-0.473124	-0.026601
146.304	235	1.541995	0.877004	0.124726	2.85926	3.702845	0.885828	0.14314	0.026183
146.304	240	1.574803	0.881952	0.132623	2.056748	2.760563	0.891869	0.081743	0.027882
146.304	245	1.607612	0.879304	0.139144	1.7771	2.361051	0.890246	0.246854	0.113938
146.304	250	1.64042	0.874349	0.141494	1.751696	2.001783	0.885722	0.149638	0.082644

	Date	Station	P_pl	P_a	T_a	P_pl corr	T_a corr	P_a corr	V_ref
			" H2O	psia	deg F	" H2O	deg C	" Hg	
1	12-Feb	sc1	11.9	14.65	64	11.8	17.77778	29.82769	71.4586
2	13-Feb	sc1	12.1	14.75	60.5	12	15.83333	30.0313	71.5658
3	20-Feb	13	12.1	14.67	62	12	16.66667	29.86841	71.8583
4	22-Feb	12	11.9	14.56	62.5	11.8	16.94444	29.64445	71.5698
5	23-Feb	1	12.1	14.65	66	12	18.88889	29.82769	72.1809
6	24-Feb	11	12.2	14.74	64	12.1	17.77778	30.01093	72.1196
7	2-Mar	sc1	2.3	14.65	58.5	2.3	14.72222	29.82769	32.887
8	2-Mar	sc1	4.5	14.65	62	4.5	16.66667	29.82769	44.934
9	2-Mar	sc1	6.95	14.65	63	6.95	17.22222	29.82769	55.299
10	2-Mar	sc1	10.05	14.65	63.5	10.05	17.5	29.82769	66.0812
11	2-Mar	sc1	13.2	14.65	63.5	13.2	17.5	29.82769	75.4189
12	8-Mar	9bl	11.8	14.8	76	11.7	24.44444	30.1331	71.6203
13	8-Mar	8bl-1	12.1	14.78	77.5	12	25.27778	30.09238	72.6541
14	8-Mar	8bl-2	12.25	14.79	75	12.15	23.88889	30.11274	72.8992
15	9-Mar	7bl	11.9	14.79	70.5	11.8	21.38889	30.11274	71.5698
16	15-Mar	7.5bl-1	11.9	14.78	68	11.8	20	30.09238	71.4243
17	16-Mar	7.5bl-2	11.9	14.74	74	11.8	23.33333	30.01093	71.9273
18	16-Mar	7.25bl-1	11.8	14.74	76.5	11.7	24.72222	30.01093	71.7951
19	16-Mar	7.25bl-2	11.9	14.74	75.5	11.8	24.16667	30.01093	72.0247
20	18-Mar	6blu	12.1	14.66	72	12	22.22222	29.84805	72.5676
21	18-Mar	5blu	12.3	14.66	74	12.2	23.33333	29.84805	73.2894
22	23-Mar	6blv	12.15	14.72	68	12.05	20	29.97021	72.5872
23	23-Mar	5blv	11.95	14.72	68	11.85	20	29.97021	71.7122

THIS PAGE INTENTIONALLY LEFT BLANK

LIST OF REFERENCES

1. Gelder, T.F., Schmidt, J.F., Suder, K.L., and Hathaway, M.D., "Design and Performance of Controlled-Diffusion Stator Compared With Original Double-Circular-Arc Stator", NASA Technical Paper 2852, March 1989.

2. Sanger, N.L., "The Use of Optimization Techniques to Design Controlled-Diffusion Compressor Blading", *ASME Journal Of Engineering For Power*, Vol. 105, pp.256-264, 1983.

3. Hansen, D.J., "Investigation of Second Generation Controlled-Diffusion Compressor Blades in Cascade", Master's Thesis, Naval Postgraduate School, Monterey, California, September 1995.

4. Schnorenberg, D.G., "Investigation of the Effect of Reynolds Number on Laminar Separation Bubbles on Controlled-Diffusion Compressor Blades in Cascade", Master's Thesis, Naval Postgraduate School, Monterey, California, June 1996.

5. Carlson, J.R., "Experimental and Computational Investigation of the End-Wall Flow in a Cascade of Compressor Blades", Master's Thesis, Naval Postgraduate School, Monterey, California, September 2000.

6. Caruso, T.M., "Three-Component LDV Measurements of Corner Vortices over Second-Generation, Controlled-Diffusion, Compressor Blades in Cascade", Master's Thesis, Naval Postgraduate School, Monterey, CA, September 2001.

7. Nicholls, J.L., "Investigation of Flow Over Second Generation Controlled-Diffusion Blades in a Linear Cascade", Master's Thesis, Naval Postgraduate School, Monterey, California, September 1999.

THIS PAGE INTENTIONALLY LEFT BLANK

INITIAL DISTRIBUTION LIST

1. Defense Technical Information Center
   Ft. Belvoir, Virginia

2. Dudley Knox Library
   Naval Postgraduate School
   Monterey, California

3. Department Chairman, Code ME
   Department of Mechanical and Astronautics Engineering
   Naval Postgraduate School
   Monterey, California

4. Dr. Garth V. Hobson, Code ME/HG
   Department of Mechanical and Astronautics Engineering
   Naval Postgraduate School
   Monterey, California

5. Dr. Raymond P. Shreeve, Code ME/SF
   Department of Mechanical and Astronautics Engineering
   Naval Postgraduate School
   Monterey, California

6. Naval Air Warfare Center
   AIR-4.4.T (Attn: Mr. C. Gorton)
   Propulsion and Power Engineering, Building 106
   Patuxent, Maryland

7. Naval Air Warfare Center
   AIR-4.4.T (Attn: Mr. R. Ravindranath)
   Propulsion and Power Engineering, Building 106
   Patuxent, Maryland

8. Naval Air Warfare Center
   AIR-4.4.T (Attn: Mr. M. Klein)
   Propulsion and Power Engineering, Building 106
   Patuxent, Maryland